

# SKBF TECHNICAL KBS REPORT

**84-02**

## **Radiolysis of concrete**

Hilbert Christensen  
Studsvik Energiteknik AB,  
Nyköping, Sweden

Erling Bjergbakke  
Risö National Laboratory,  
Roskilde, Denmark 1984-03-16

## RADIOLYSIS OF CONCRETE

Hilbert Christensen  
Studsvik Energiteknik AB  
Nyköping, Sweden

Erling Bjergbakke  
Risö National Laboratory  
Roskilde, Denmark

1984-03-16

This report concerns a study which was conducted for SKBF/KBS. The conclusions and viewpoints presented in the report are those of the author(s) and do not necessarily coincide with those of the client.

A list of other reports published in this series during 1984 is attached at the end of this report. Information on KBS technical reports from 1977-1978 (TR 121), 1979 (TR 79-28), 1980 (TR 80-26), 1981 (TR 81-17), 1982 (TR 82-28) and 1983 (TR 83-77) is available through SKBF/KBS.

1984-03-16

Hilbert Christensen  
Erling Bjergbakke

SKBF/KBS

## RADIOLYSIS OF CONCRETE

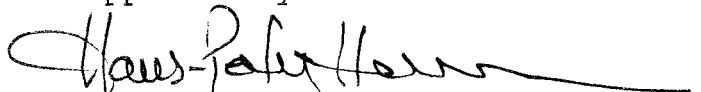
A computer based radiation chemical program has been used to simulate experiments with gamma and alpha radiolysis in concrete. The experiments have been performed at Savannah River by Ned Bibler and co-workers. The calculations showed that the gas yields were very sensitive to the pH of the water phase. At a pH of 12.3 fairly good agreement was obtained between measured and calculated gas yields, assuming that the gas production only took place in the free water phase of the concrete. The following main conclusions could be made from both measurements and calculations:

- 1) A steady state is obtained by gamma radiolysis of a  $\text{NO}_3^-$  free concrete.
- 2) The yields are higher and a steady state is not obtained if  $\text{NO}_3^-$  is present.
- 3) The yields are higher and a steady state is not obtained by alpha radiolysis.

Calculations were also carried out on radiolysis from cladding hull waste stored in a cement matrix assuming both alpha and beta radiation. In the presence of an aerated gas phase a steady state pressure of more than 0.21 MPa was obtained.

\*Risö National Laboratory, Risö,  
DK-4000 Roskilde, Denmark

Approved by



## CONTENTS

	<u>Page</u>
1. INTRODUCTION	3
2. COMPUTER MODEL	4
2.1 Computer program	4
2.2 Presence of gas phase	5
2.3 Primary yields of radiolysis products	6
3. COMPARISON WITH MEASUREMENTS	6
3.1 Introduction	6
3.2 Effect of pH	7
3.3 Test cases	8
3.3.1 Gamma irradiation	8
3.3.2 Alpha irradiation	12
3.3.3 Combined alpha and gamma irradiation	15
3.3.4 Effect of $\text{NO}_3^-$	16
3.4 Conclusions	18
4. RADIOLYSIS IN CEMENTED CLADDING HULLS	20
4.1 Activity content and dose rates	20
4.2 Results of calculations	21
5. CONCLUSIONS	23
REFERENCES	26
TABLES	28
APPENDIX 1	35

## 1. INTRODUCTION

One of the waste products from reprocessing is fuel cladding hulls which is planned to be encapsulated in cement. Radiolysis is an important aspect for the safety of the storage of this product. Concrete has been considered as the storage form for defense waste in USA, and an experimental programme, including radiolysis studies, has been carried out, primarily at the Savannah River Laboratory, SRL (1, 2).

Bibler at SRL has studied the gas production from the radiolysis of concrete, by external and internal gamma or alpha irradiation for different types of waste. The conclusions from Bibler's studies are that hydrogen is produced from both gamma and alpha radiolysis. Oxygen is produced in alpha radiolysis but it is normally consumed in gamma radiolysis. A steady state is obtained from gamma radiolysis. The steady state concentration is proportional to the square root of the dose rate. Gas production by alpha radiolysis continues with a constant G-value. Pressures of up to 1.4 MPa have been measured, and based on this a pressure exceeding 14 MPa has been calculated to exist after a storage time of  $10^5$  year (2). Steady state concentrations were not achieved by gamma irradiation at higher dose rates ( $2.8 \times 10^7$  rad/h) in the presence of  $\text{NO}_3^-$  or  $\text{NO}_2^-$ .

We have made calculations simulating the conditions in Bibler's experiments in order to check whether the radiolysis in concrete can be described by radiolysis of the water phase in the concrete.

In addition we have made calculations of radiolysis in concrete under storing conditions anticipated for Swedish waste.

Radiolysis in water of crystallization has not been considered here, but has been described in a separate report by Z P Zagorski (3). Zagorski's report has been included as Appendix 1 of the present report.

Radiolysis of concrete containing organic waste has not been considered here.

## 2. COMPUTER MODEL

### 2.1 Computer program

We have used a computer program based on DIFSUB (7) and developed by Lang-Rasmussen, Risö, Denmark. In principle the program translates the chemical equations of the complete reaction system into a set of differential equations, which is solved by numerical integration after specifying of rate constants, initial concentrations, G-values, irradiation dose and duration. The results are presented in tables giving the concentrations of the various species at various times during, and even after, the irradiation (if wanted). As an option, the results can also be presented as curves showing the concentrations as a function of time.

As input data the program requires

- a) a list of all the chemical reactions involved,
- b) rate constants for these reactions,
- c) G-values for all the primary products,
- d) initial concentrations of all species at the start of irradiation,

e) dose and duration of the irradiation.

a) and b) are shown in Table 3.

The predictive capacity of the program has been tested by comparing calculations with results of measurements by T Eriksen and J Lind (8). Eriksen and Lind irradiated bentonite/water mixtures to various doses and measured the hydrogen production in the gas phase. The hydrogen was analysed by gas chromatography.  $O_2$  and  $H_2O_2$  were not determined in the experiments. The correlation between measured and calculated results was very good (4). Calculated results have also been compared with literature data. In this case the correlation was also very good (9).

In the presence of iron,  $NO_2^-$ , and  $NO_3^-$  ions the reactions listed in Table 4 have been included in the mechanism.

## 2.2 Presence of gas phase

The program is designed for a homogeneous liquid phase. However a gaseous phase can be simulated by using two elements: Dummy I and II, which represent  $H_2$  and  $O_2$  in the gaseous phase, but which the program treats as components in the liquid phase. Equations 37-41 describe the partition between the liquid and gaseous phases: equations 37 and 40 apply to  $H_2$  and 39 and 41 to  $O_2$ . The relationship between the volumes of gas and liquid have been taken in account. The ratios  $K_{37}/K_{40}$ , and  $K_{39}/K_{41}$  are determined by the solubility of hydrogen and oxygen respectively. The absolute values have been taken to be large so that the equilibrium between the liquid and gaseous phases will be established quickly.

From equations 37 and 40 it can be seen that at equilibrium

$$K_{37}/K_{40} = \frac{(\text{Dummy I})}{(\text{H}_2)_{\text{liq}}} = K$$

$$(\text{Dummy I}) = (\text{H}_2)_{\text{gas}} \times \frac{V_{\text{gas}}}{V_{\text{liq}}}$$

$$K_{37} = K_{40} \times K_D \times \frac{V_{\text{gas}}}{V_{\text{liq}}}$$

### 2.3 Primary yields of radiolysis products

The primary yields of radiolysis products discussed and applied previously (4) have been used and are summarized in Table 1.

## 3. COMPARISON WITH MEASUREMENTS

### 3.1 Introduction

Bibler has presented results from radiolysis experiments under different conditions (1, 2). In the following results from calculations are compared with the experimental values for 12 cases. They include experiments with pure gamma-irradiation, pure alpha-irradiation and combinations of alpha and gamma-irradiation. The effect of  $\text{NO}_3^-$ -ions is also included.

As far as possible the data given by Bibler have been used. In some cases the initial conditions were not specified directly in Bibler's reports, but could be inferred.

All the experiments were carried out in closed containers assuming an initial air pressure of 1 atm.



### 3.2 Effect of pH

The pH of concrete is normally in the range of 12.5 - 13.5. In the beginning pH is about 13 and is determined by NaOH and KOH. Later on the pH is determined by CaOH and is then 12.6. However, contents of  $\text{SiO}_2$  and other oxides may decrease the pH. In the first calculations a pH of 13 was assumed. However, the calculated results were not in good agreement with the experiments (case 1 below). Therefore the results of calculations carried out at various values of pH (7, 12.0, 12.3, 12.7 and 13) were compared. It can be seen from Figs 1-2 that the pH is an important parameter. This is because of the changes in the rate constants with pH, mainly K3, K8, K14 and K15. The species OH and  $\text{H}_2\text{O}_2$ , which exist in neutral and acid solutions, are substituted by  $\text{O}^-$  and  $\text{HO}_2^-$  in alkaline solutions, the pK being about 11.9 for both species (10). The species  $\text{O}^-$  and  $\text{HO}_2^-$  react with other rate constants than the species OH and  $\text{H}_2\text{O}_2$ .

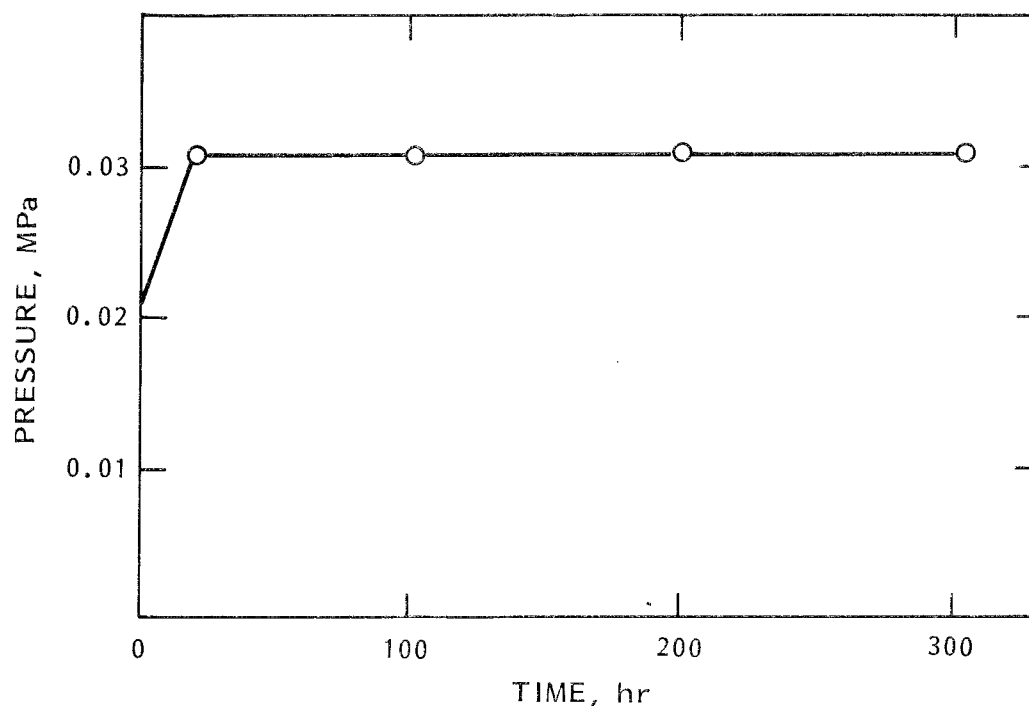


Figure 1. Calculated results for case 1 at a pH of 7.0

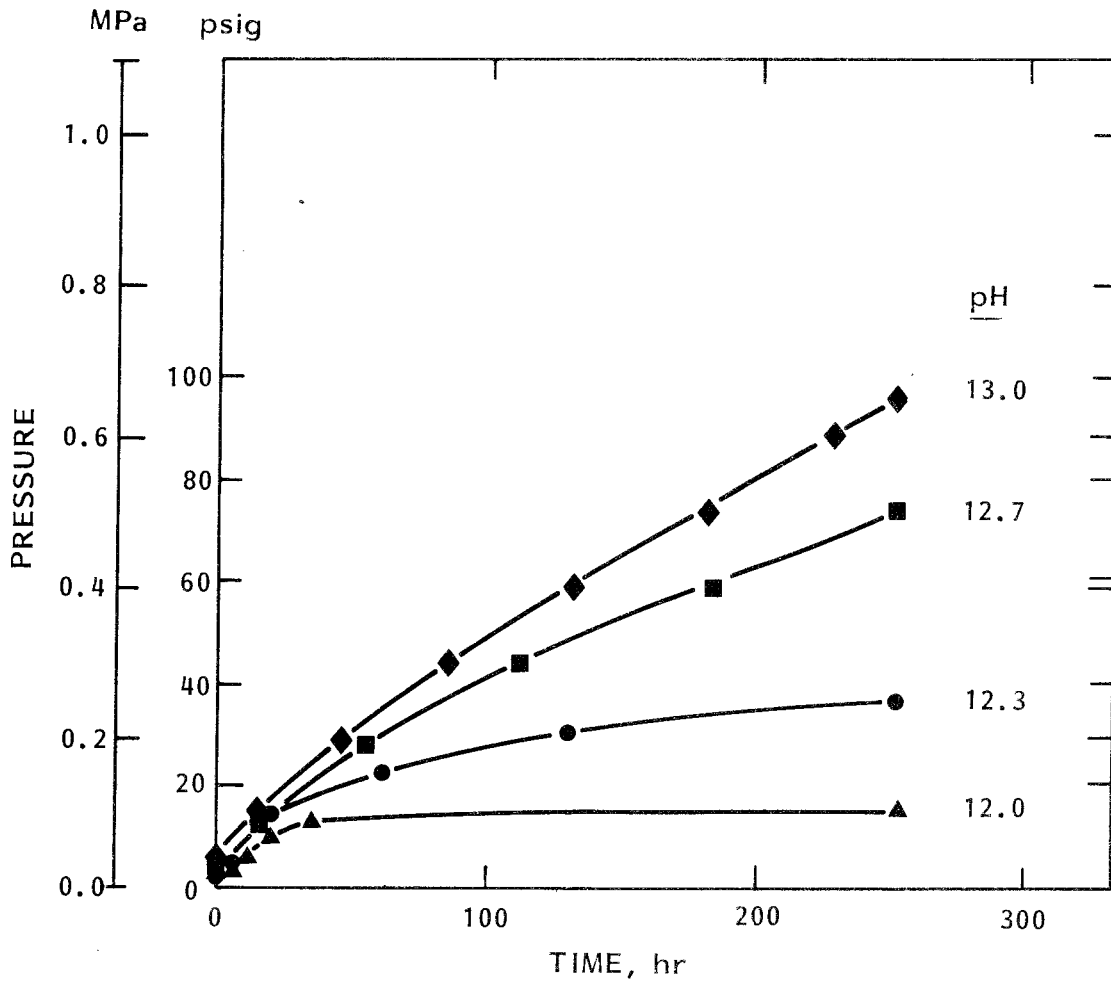


Figure 2. Calculated results for case 1 as a function of pH.

The best agreement was obtained using a pH of 12.3. Therefore, we have assumed this pH to be relevant for the experiments and used it in all subsequent calculations.

### 3.3 Test cases

#### 3.3.1 Gamma irradiation

Case 1 and 2

Portland cement and gypsum perlite based concrete. Experiments described in Ref 1, Fig 1.

### Conditions and results

	Case 1	Case 2
Water volume, ml	65*	61*
Gas volume, ml	168	112
Dose rate (gamma), rad/h	1.4E7	2.6E7
Irradiation time(expt), h	400	400
" " (calc), h	800	800
Pressure after 400h(expt), MPa	0.23	0.31
" " (calc), "	0.25	0.25

\* This is a reduced water volume used in the calculations. The reduction is 25% which is motivated by reactions and water of crystallization, which is assumed not to take part in the radiolysis.

Measurements and calculations can also be seen in Figure 3.

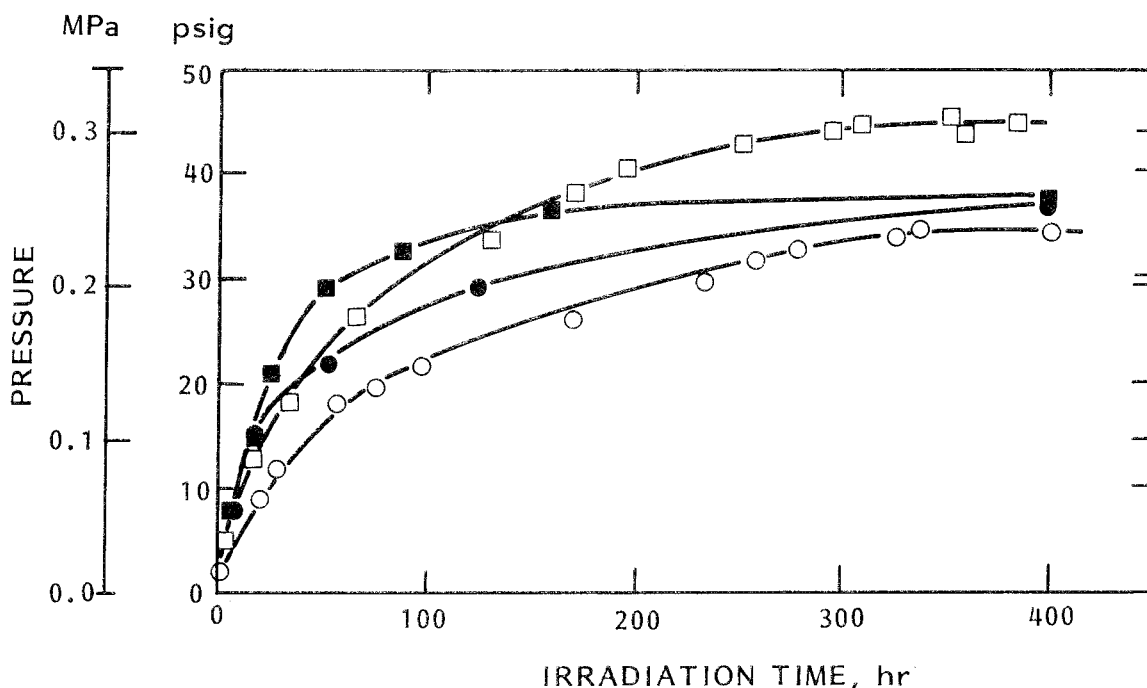


Figure 3. Gamma radiolysis.

Pressurization from gamma radiolysis of concrete at 47°C.

Experimental results (From DP-1459, Fig. 1):

○ =:  $1.4 \times 10^7$  rad/h, □:  $2.6 \times 10^7$  rad/h.

Calculated results: ●:  $1.4 \times 10^7$  rad/h (case 1);

■ :  $2.6 \times 10^7$  rad/h (case 2).

In the calculations, stoichiometric amounts of hydrogen and oxygen are formed. In the experiments oxygen in the air trapped in the container was partially consumed and  $N_2$  was unaffected.

The calculated curves agree fairly well with the experimental curves, however the difference in the calculated final pressures is small in the two cases.

We have also made calculations in order to determine the effect of dose rate: Case 1 was repeated but with 10 and 100 times lower dose rates (389 and 39 rad/s, respectively). As can be seen from Table 8, the equilibrium pressure appears to be independent of dose rate, contrary to the experimental findings.

#### Case 3-6

Experiments described in Ref 2, Table 2 and Fig 3.

#### Conditions and results

	Case 3	Case 5	Case 4	Case 6
Water volume, ml	55	55	55	55
Gas " , ml	167	167	167	167
Gamma dose rate, rad/h	2.8E7	2.8E7	2.5E7	2.5E7
Irradiation time, h				
- experiment				260
- calculations	560	560	560	560
Iron conc ( $Fe^{3+}$ ), $\mu M$	0	1	0	1
Measured equil pressure, MPa		0.72		0.83
Calculated equil pressure, MPa	0.26	0.25	0.26	0.24

Measured and calculated results are shown in Figure 4. The yields are a little lower in the presence of iron.

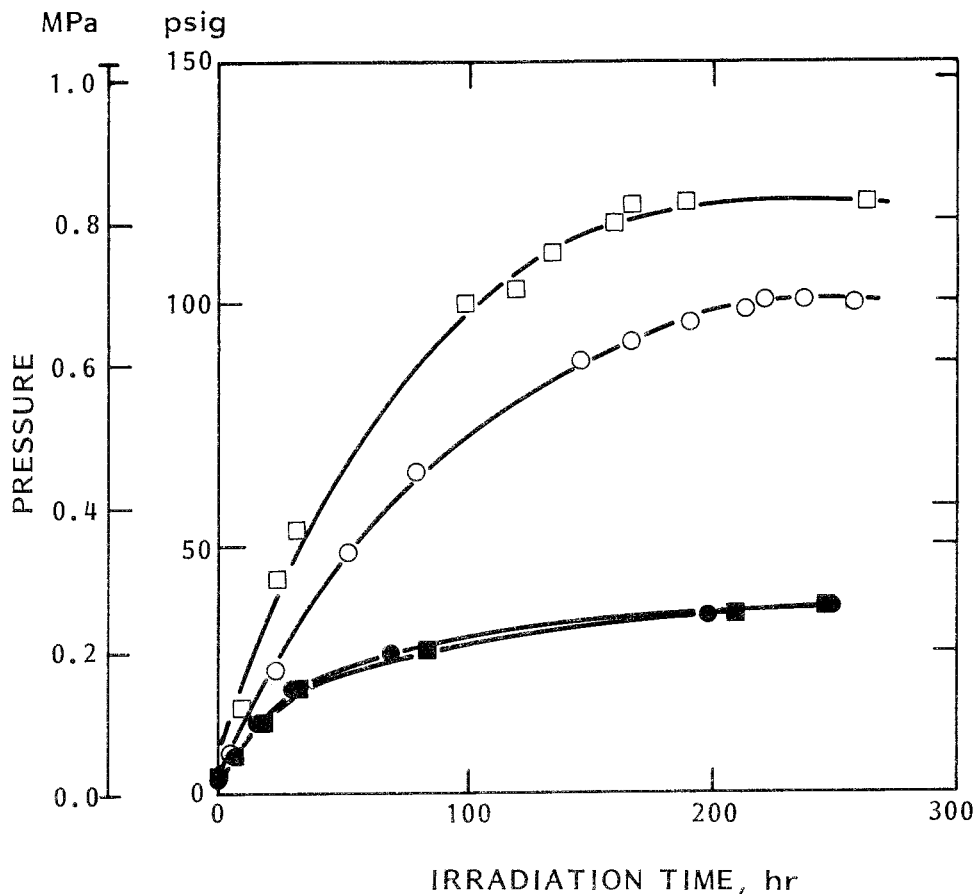


Figure 4. Gamma radiolysis

Pressure from gamma radiolysis at two dose rates of concrete containing  $\text{Fe}_2\text{O}_3$ .

Experimental results (From DP-1464, Fig.3)

○:  $1.4 \times 10^7$  rad/h; □:  $2.5 \times 10^7$  rad/h.

Calculated results: ●:  $2.8 \times 10^7$  rad/h (case 3);

■:  $2.5 \times 10^7$  rad/h (case 4).

In the calculations stoichiometric amounts of hydrogen and oxygen are formed. This was not always the case in Bibler's experiments, indicating that some unknown (oxygen consuming) reactions were taking place.

## 3.3.2 Alpha irradiation of concrete

$^{244}\text{Cm}$  is used as an internal alpha-source.

## Case 7

Experiment described in Ref 1, Figure 4.

Conditions and results

Water volume, ml	3.5
Gas volume, ml	11.6
Alpha dose rate, rad/h	2.8xE6
Irradiation time, h	
- experiment	330
- calculations	700
Measured pressure after 330 h, MPa	1.39
Calculated " " " , MPa	1.13
Calculated pressure after 330 h including decomposition of $\text{H}_2\text{O}_2$ to $\text{O}_2$ , MPa	1.39

In both the measurements and the calculations the pressure increased at a constant rate, see Figure 5.

The calculated hydrogen peroxide concentration after 330 h was 0.725 M, which is probably an unrealistically high concentration.  $\text{H}_2\text{O}_2$  is probably decomposed to oxygen through catalytic reactions.

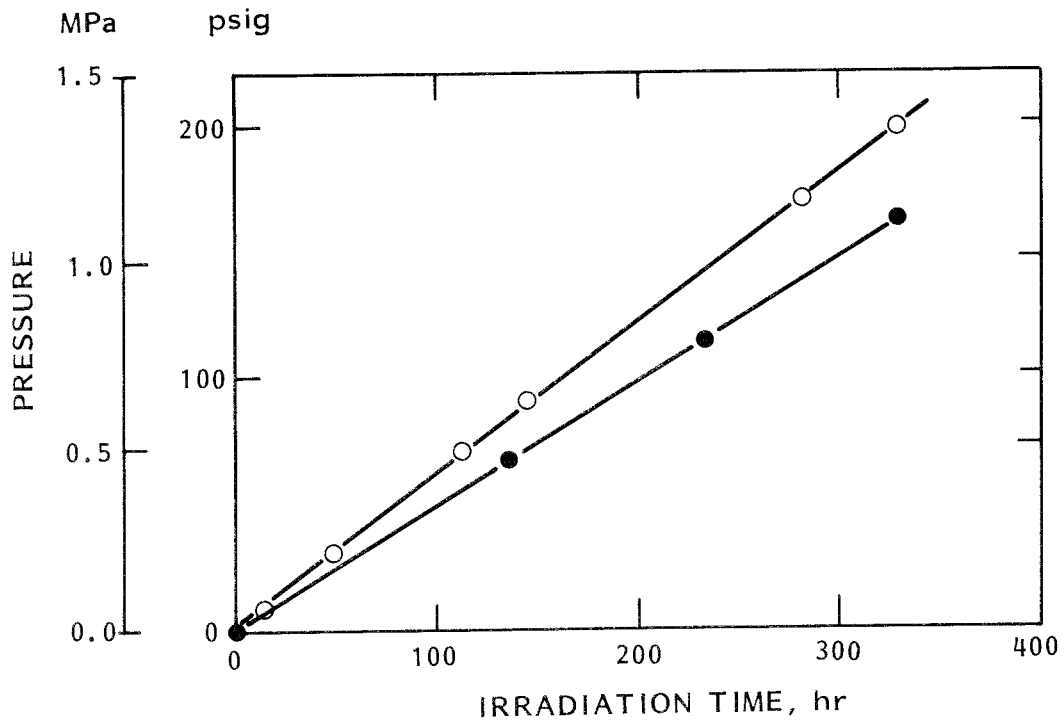


Figure 5. Alpha radiolysis.

High pressure generated from alpha radiolysis of concrete at 23°C.

Experimental results (From DP-1459): O

Calculated results (case 7): ●

## Case 8

Experiment described in Ref 2, Figure 13.

Conditions and results

Water volume, ml	3.4
Gas " , ml	9
Alpha dose rate, rad/h	2.7xE5
Irradiation time, h	
- experiment	3670
- calculations	8000
Measured pressure after 3670 h, MPa	1.33
Calculated " " , MPa	1.47
Calculated pressure after 3670 h including O <sub>2</sub> from decomposition of H <sub>2</sub> O <sub>2</sub> , MPa	1.83

Measured and calculated results can be compared in Figure 6.

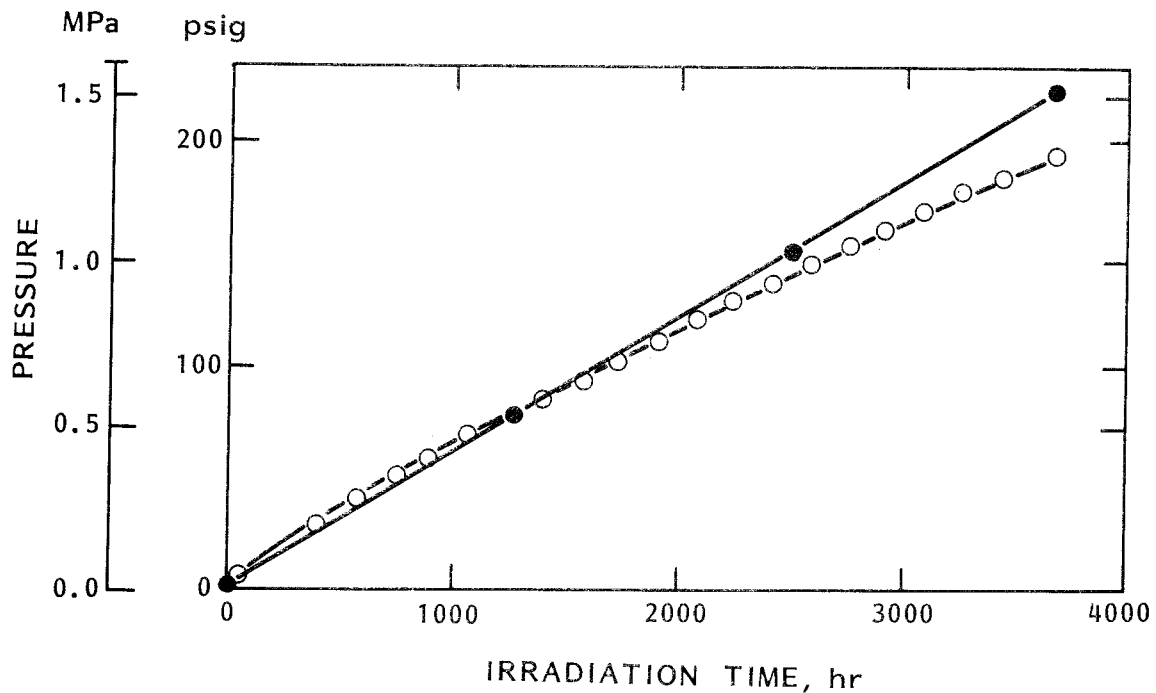


Figure 6. Alpha radiolysis.

Pressure from Long-Term Alpha Radiolysis of Concrete Container Fe-Mn Simulated SRP Waste.  
Experimental results (From DP-1464): ○  
Calculated results (case 8): ●



Stoichiometric formation of oxygen and hydrogen was found both in experiments and in calculations. In both cases 7 and 8 the pH decreased from 12.3 to 10.2. In both cases 7 and 8 the G-value for the hydrogen production was 1.29, if the calculation is based only on the radiation absorbed in the water phase.

### 3.3.3 Combined alpha and gamma irradiation

#### Case 9

Experiment described in ref 2, p 28-29. 165 g concrete containing actual SRP waste (SRP: Savannah River Plant) was used.

#### Conditions and results

Water volume, ml	82
Gas volume, ml, aerated	167
Dose rate, rad/h	gamma: $3 \times 10^4$
" " "	alpha: $4 \times 10^2$
Irradiation time:	
- experiment, y	1
- calculations, y	2

Bibler's results and the corresponding calculated results are presented in Figure 7. After one year both containers leaked. The calculated pressure after 1 y was 0.11 MPa and the measured pressure was 0.05 MPa. After 250 d the calculated pressure was 0.09 MPa and the measured pressure was 0.05 MPa. A possible explanation for the differences may be the uncertainty in pH or water volume.

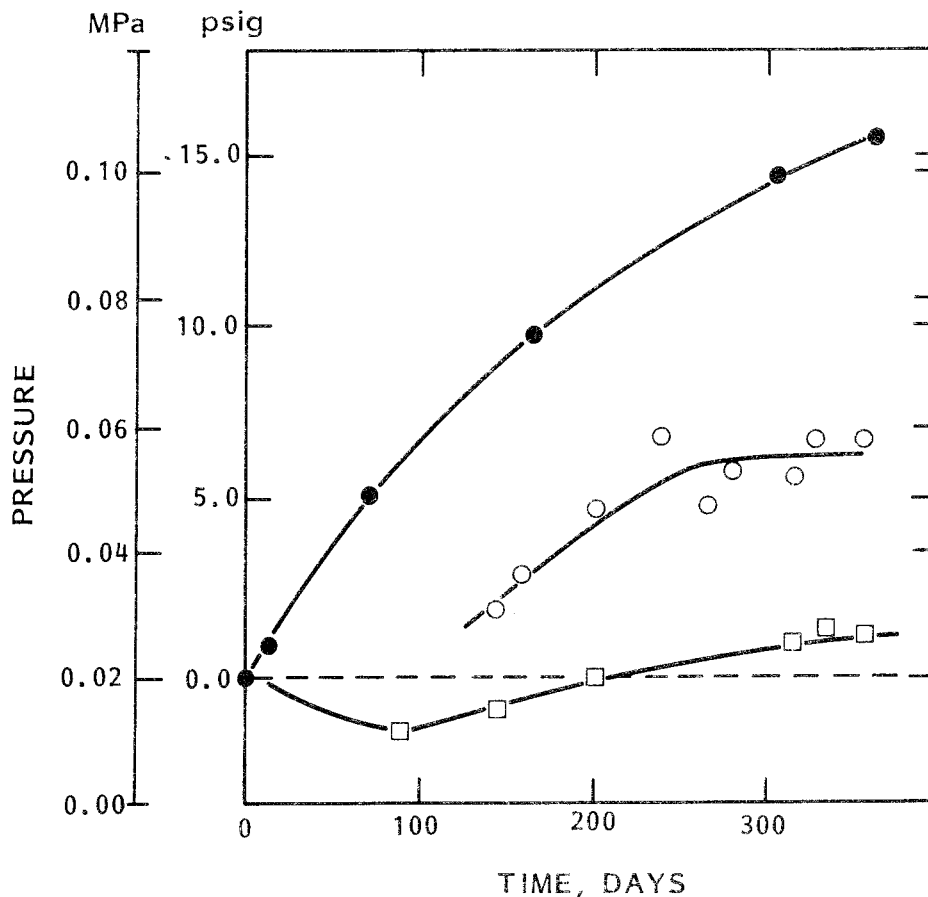


Figure 7. Radiolysis in waste containers.

Pressure from Concrete Containing Radioactive SRP Waste.

Experimental results from two containers (From DP-1464): ○, □

Calculated results (case 9): ●

The contribution of alpha radiation is only about 1% in this case.

The composition of the gas in the experiments is not given. In the calculations stoichiometric amounts of oxygen and hydrogen are formed.

### 3.3.4 Gamma irradiation of concrete containing $\text{NO}_3^-$ and/or $\text{NO}_2^-$

Case 10-12

Experiments described in Ref 2, Figure 7.

Conditions and results

	Case 10	Case 11	Case 12	Case 5
Water volume (assumed), ml	55	55	55	55
Gas volume (assumed), ml	167	167	167	167
Gamma dose rate, rad/s	2.8E7	2.8E7	2.8E7	2.8E7
Iron conc, $\mu\text{M}$ in water	1	1	1	1
$\text{NO}_3^-$ , wt% of concrete	1	5	5	0
$\text{NO}_2^-$ , " " "	0	0	2.5	0
Irradiation time, h	143	143	143	143
Measured pressure, MPa	1.28			
Calculated " , MPa	2.34	2.54	2.28	0.22

The results are shown in Figure 8.

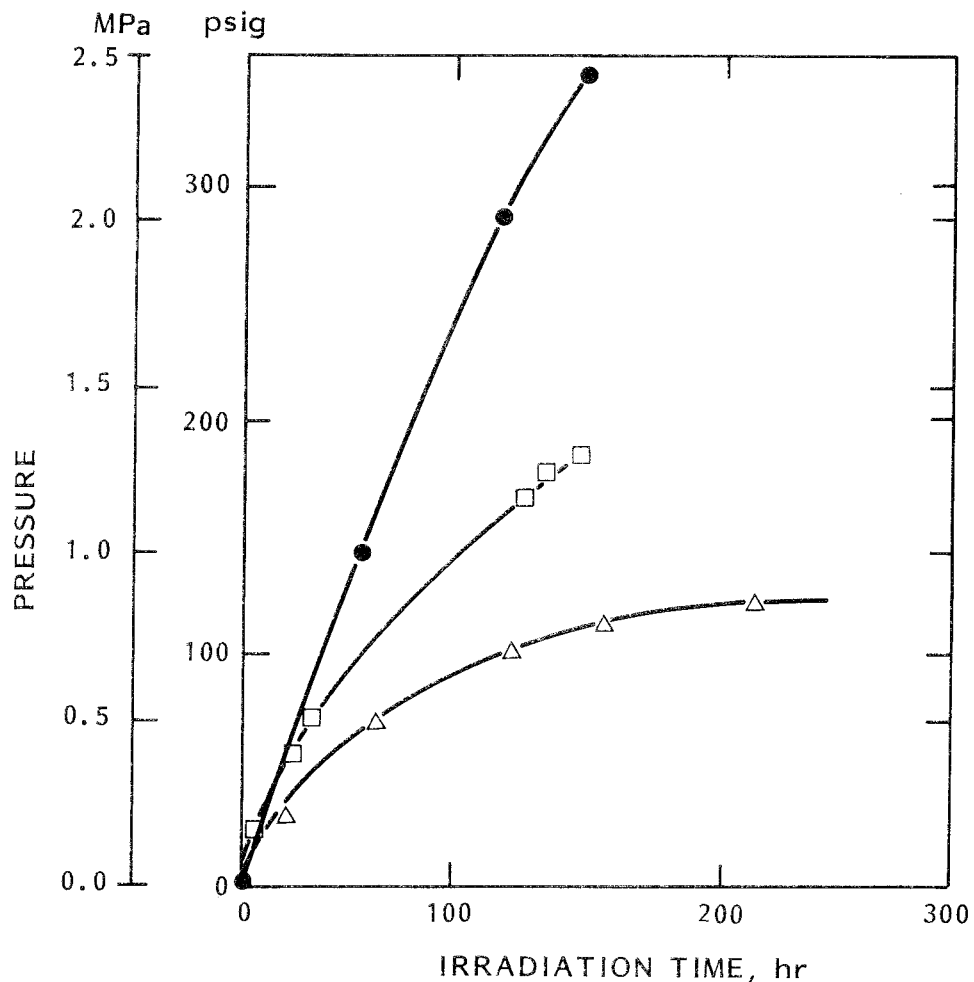


Figure 8. Effect of  $\text{NO}_3^-$ .

Pressure from gamma radiolysis at  $2.8 \times 10^7$  rads/hr of concrete containing  $\text{Fe}_2\text{O}_3$  with sorbed  $\text{NO}_3^-$  ions. Experimental results (From DP-1464):  $\square$  : 1%  $\text{NO}_3^-$ ;  $\triangle$  : 0%  $\text{NO}_3^-$ . Calculated results (case 10):  $\bullet$  : 1%  $\text{NO}_3^-$

Both experiments and calculations show a considerable effect of  $\text{NO}_3^-$  on the gas production, which is much higher in the presence of  $\text{NO}_3^-$ . It should be noted that a steady state is not obtained in the presence of  $\text{NO}_3^-$ .

Almost stoichiometric amounts of hydrogen and oxygen are formed in addition to small yields of nitrogen oxides.

The calculated pressure (case 10) is higher than the measured pressure. The difference could be caused by a lower pH in the experiment than is to be expected (if acid nitrates are added to the concrete). We have interpreted Bibler's description of the experiment to mean  $\text{NO}_3^-$  contents of 1 and 5 wt% of the concrete, and have then assumed the concentrations in the water phase to be 3 times higher.

### 3.4 Conclusions

The comparisons between Bibler's measurements and our calculations show that the latter can describe the principles derived in the measurements:

- 1) A steady state is obtained by gamma radiolysis of a  $\text{NO}_3^-$ -free concrete
- 2) The yields are higher and a steady state is not obtained if  $\text{NO}_3^-$  is present
- 3) The yields are higher and a steady state is not obtained by alpha radiolysis.

In some cases we have calculated lower and in other cases higher yields than found in the experiments. It has been shown that the gas

yields are very sensitive to the pH in the water phase of the concrete, which must consequently be known accurately. Other important parameters are type of radiation, dose, initial concentrations of  $\text{NO}_3^-$ ,  $\text{O}_2$ , and organics, type of organics, and - especially for alpha irradiation - the gas/liquid ratio.

Obviously, in the experiments there is an unknown oxygen consuming process. Radiolysis of pure water yields stoichiometric quantities of oxidizing and reducing species. An oxygen consumption may be caused by organics or  $\text{Fe}^{2+}$  ions. Despite the excess of hydrogen found in the experiment we obtain roughly the same pressure in experiments and calculations. It might be possible to include oxygen consuming reactions and at the same time change the pH in the calculations and thus obtain another fit to the experiments.

As can be seen from Table 1 the radical yields ( $e_{\text{aq}}^-$ , H and OH) are much larger and the molecular yields ( $\text{H}_2$  and  $\text{H}_2\text{O}_2$ ) much lower for gamma radiation, in comparison with alpha radiation. Therefore, the recombination reactions 8, 14 and 16 are important for gamma irradiation. The result of these reactions is that a steady state is obtained. Scavengers, which react with the radicals and thus impede the recombination, may change the situation drastically. This can be seen in the cases where  $\text{NO}_3^-$  is added. If the recombination is blocked totally a  $G(\text{H}_2)$  value of 0.5 would be expected. Due to the low yields of radicals in alpha irradiation, scavengers are not expected to have a great effect in this case.

Stoichiometric amounts of hydrogen and oxygen are formed according to the calculations, but only hydrogen was found in the gamma-experiments in the absence of  $\text{NO}_3^-$ .

#### 4. RADIOLYSIS IN CEMENTED CLADDING HULLS

##### 4.1 Activity content and dose rates

Dose rates in the cemented cladding hulls were calculated using the following information, (5):

1 ton U gives 300 kg cladding hull waste containing: 6000 Ci activation products, mainly  $^{60}\text{Co}$  and  $^{55}\text{Fe}$ , 10000 Ci fission products, mainly  $^{106}\text{Ru}$  and 0.1% of the fuel, i.e. about 1000 Ci, including alpha activities. These activities give a gamma and beta dose rate of 8.5 rad/s (in 3 year old waste) if the radiation is absorbed homogeneously in the concrete.

1 ton U was contained in 354 fuel pins. If the 0.1% fuel is assumed to cover the inside of the fuel cladding uniformly, a  $2 \times 10^{-4}$  cm thick layer is obtained over an area of  $4 \times 10^5$  cm<sup>2</sup>. Further the alpha irradiation is assumed to be absorbed in a 0.03 mm thick water layer, corresponding to 1.3 l. The 0.1% fuel develops a power of 0.18 W after 40 y, 50% of which is assumed to be absorbed in the water layer, corresponding to an alpha dose rate of 7 rad/s. The corresponding beta dose rate is assumed to be 2.5 rad/s, in accordance with the calculations of Klas Lundgren (6). The dose rates after various storage times are given in Table 2; they have been calculated based on data from Lundgren (6).

#### 4.2 Results of calculations

We have calculated the results of alpha radiolysis (including a contribution of beta radiolysis), in a thin water layer on the inside of the fuel cladding (1.3 l) for various times up to  $10^5$  y, see Table 5. It was assumed that hydrogen and oxygen could diffuse out of the system. The diffusion rate constants used are those valid for water ( $1.34 \times 10^{-4} \text{ s}^{-1}$  and  $4.78 \times 10^{-5} \text{ s}^{-1}$  for  $\text{H}_2$  and  $\text{O}_2$  respectively (11)).

Initially the water was assumed to be deaerated and to have a pH of 12.3. At each storage time (Table 5) calculations were carried out to simulate irradiation for at least 4 months, during which production rates were constant. The results from fuel irradiation are given in Table 5. If the yields are integrated, substantial amounts of gas are obtained ( $60 \text{ m}^3$  after  $10^5$  y).

However, it is most likely that the hydrogen and oxygen produced in the thin alpha irradiated water layer (1.3 l) diffuse into the bulk water (190 l for concrete waste from 1 ton  $\text{UO}_2$ ). Therefore we have carried out calculations on beta irradiation of the bulk water, including a continuous supply of hydrogen and oxygen produced in the thin water layer. The effect of the beta irradiation in the bulk water phase is to recombine the hydrogen and oxygen produced in the thin layer. The resultant total gas production is therefore decreased due to the effect of beta irradiation, see Table 6a, which shows that the yield of hydrogen is very low. In this calculation we have neglected the gaseous phase, and instead assumed that oxygen and hydrogen diffuse out of the system through a surrounding

bentonite layer, where the diffusion coefficients are very low, approximately 700 times lower than in water (12). The production values given in Table 6a would therefore be approximately 700 times higher if hydrogen disappeared by diffusion in water instead of in bentonite.

In the calculations shown in Table 6a it was assumed that the water was oxygen free initially. If it is assumed that the water is aerated at a pressure of 0.1 MPa the results shown in Table 6b and 6c, corresponding to diffusion through bentonite and water respectively, are obtained. In these cases (6b and 6c) it is also assumed that the system is surrounded by aerated water.

As can be seen from Tables 6a-c the initial oxygen concentration in the irradiated water phase is a very important parameter.

We have also carried out a calculation, in which we have assumed that the 190 l free water is in equilibrium with a gaseous phase of 100 l inside the concrete. Even in this case hydrogen and oxygen are supplied to the system from the thin alpha irradiated water layer. The results of this calculation are shown in Table 7. The steady state pressure is surprisingly low, when compared with Bibler's measurements and corresponding calculations, see for example Case 1.

The main differences from Case 1 are a different dose rate (Case 1: 3.890 rad/s; cladding hull waste, 3-4 y; 5.5 rad/s) and a different initial oxygen concentration (Case 1: air-saturation assumed; cladding hull waste, deaerated conditions assumed). Therefore further calculations have been made in order to explain the low equilibrium pressure obtained at steady state.



The water phase (190 l) was irradiated in the presence of an air-saturated gas phase (100 l). After 3.7 y irradiation  $/H_2/gas$  was  $5.51 \times 10^{-2} M$ , corresponding to a pressure of 1.3 atm (19 psig). The total pressure increase was 2.0 atm (28 psig), see Table 7; the gas pressure was still not at its equilibrium value. It is obvious from this calculation that an initial presence of oxygen is very important for the formation of gases from the radiolysis of water.

## 5. CONCLUSIONS

The gas yields are very sensitive to the pH of the water phase. At a pH of 12.3 a fairly good agreement was obtained between measured and calculated yields, assuming radiolysis of the free water phase only.

The gas yields are very sensitive to the initial oxygen concentration. The yields are approximately  $10^3$  times higher in aerated conditions compared with deaerated conditions.

The following main principles were found in both measurements and calculations:

- 1) A steady state is obtained by gamma radiolysis of a  $NO_3^-$ -free concrete.
- 2) The yields are higher and a steady state is not obtained if  $NO_3^-$  is present.
- 3) The yields are higher and a steady state is not obtained by alpha radiolysis.

In the measurements it was found that during gamma radiolysis the steady state pressure was proportional to the square root of the radiation intensity.

In the calculations it was found that during gamma radiolysis the steady state pressure was independent of dose rate in the range 39-3890 rad/s.

It is possible that some reactions take place in the experiments which have been disregarded in the calculations. The square root law was obtained partly by pressurization with hydrogen, which, however, may change the result of the irradiation.

Studies carried out by Zagorski, pages 9 and 20 of ref (3) indicate that radiolysis in water of crystallization is unimportant for the production of the gases.

Experiments of Möckel and Köster (13) also indicate that chemically bonded hydrate-water is less susceptible to radiolysis than the bulk water.

Möckel and Köster have found that hydrogen alone is formed by gamma-radiolysis of  $\text{NO}_3^-$  free cement. In the presence of 10%  $\text{NaNO}_3$  the hydrogen production is reduced by a factor of 10 and the gas produced consists to more than 60% of oxygen. No nitrogen oxides are formed. Möckel and Köster added fluidizer to the concrete. M & K also remark that the yield of  $\text{H}_2$  increases linearly with dose, i.e. saturation is not observed, dose rate  $(2.5-4.9) \times 10^5$  rad/h, dose  $(0.7-9) \times 10^{22}$  eV.

The gas production in Bibler's experiment seems to be independent of the w/c ratio (at ratios of 3-4). The calculated steady state pressure is also independent of the w/c ratio. However, the initial rate of production found in the calculations is dependent on this ratio.

Möckel and Köster (13) have found an increasing hydrogen yield with increasing w/c ratio (in the range w/c 0.2-0.6).

A possible presence of organic material in the waste product might explain the preferential formation of hydrogen found in Bibler's gamma-irradiation experiments. The presence of  $\text{Fe}^{2+}$  ions may have the same effect.

## REFERENCES

1. BIBLER N E and OREBAUGH E G,  
Radiolytic gas production from tritiated  
waste forms.  
Report DP-1459, Savannah River Labora-  
tory, Aiken, SC, 1977.
2. BIBLER N E,  
Radiolytic gas production from concrete  
containing Savannah River Plant waste.  
Report DP-1464, Savannah River Labora-  
tory, Aiken, SC, 1978.
3. ZAGORSKI Z P,  
Electrons trapped in crystalline  
systems containing water.  
Studsvik Technical Report NW-83/416,  
(1983-01-25).
4. CHRISTENSEN H and BJERGBAKKE E,  
Radiolysis of ground water from spent  
fuel.  
Studsvik Report NW-82/364.
5. FORSSTRÖM H,  
Personal communication, Dec 1982.
6. LUNDGREN K,  
Strålningsnivå och till vatten deponerad  
strålningsenergi utanför kapslar i  
slutförvaret. (In Swedish)  
KBS TR 106(1978).
7. GEAR C W,  
Algorithm 407, DIPSUB, Commun. ACM,  
1971, 14, 185.
8. ERIKSEN T and LIND J,  
Mätning av radiolytiskt bildat vätgas i  
bentonit. (In Swedish)  
KBS TR 79-13 (1979).
9. BJERGBAKKE E,  
Computer simulations control.  
Private communication, 1981-08-28.
10. CHRISTENSEN H, SEHESTED K and CORFITZEN H,  
Reactions of hydroxyl radicals with  
hydrogen peroxide at ambient and  
elevated temperatures, J Phys Chem  
1982, 86, 1588.
11. CHRISTENSEN H and BJERGBAKKE E,  
Radiolysis of ground water from HLW  
stored in copper canister.  
KBS TR 82-02 (1982).

12. NERETNIEKS I and SKAGIUS E,  
Diffusioismätningar av metan och väte i  
våt lera. (In Swedish)  
KBS TR 86 (1978).
13. MÖCKEL H J and KÖSTER R H,  
Gas formation during the gamma-radio-  
lysis of cemented low- and inter-  
mediate-level waste products.  
Nucl Techn 59, 494-97 (1982).

TABLE 1. Primary G-values by irradiation of water

	$\alpha$	$\gamma$ and $\beta$	$\alpha + \beta$
			(thin water layer)
H <sub>2</sub>	1.3	0.49	1.08
H	0.21	0.44	0.27
e <sup>-</sup>	0.06	2.68	0.75
HO <sub>2</sub> <sup>-</sup>	0.985	0.74	0.92
O <sup>-</sup>	0.24	2.59	0.86
O <sub>2</sub> <sup>-</sup>	0.22	0.01	0.16
H <sup>+</sup>	1.505	6.11	2.71
OH <sup>-</sup>		0.09	0.02
-H <sub>2</sub> O	2.71	6.86	3.79

TABLE 2. Dose rates in the water phases of the cemented cladding hull waste

Storage time	Thin water layer (1.3 l) irradiated from fuel Dose rates in rad/s		Free water in the concrete Dose rates in rad/s
	$\alpha$	$\beta$	$\beta$
3	7	2.5	8.5
40	7	2.5	2.5
100	5.75	1.73	1.73
10 <sup>3</sup>	1.75	5.3E-1	0.53
10 <sup>4</sup>	0.38	1.1E-1	0.11
10 <sup>5</sup>	1.88E-2	4.3E-3	4.3E-3

TABLE 3. Reaction scheme

	<u>Rate constant</u> <u>M<sup>-1</sup> s<sup>-1</sup></u>
RE1: $2E^- = 2OH^- + H_2$	5E9
RE2: $E^- + OH = OH^- + H_2O$	3E10
RE3: $2OH = H_2O_2$	4.5E9
RE4: $OH + O_2 = O_2^- + OH^-$	1.2E10
RE5: $OH^- + H = E^-$	2E7
RE6: $E^- + H^+ = H + H_2O$	2.4E10
RE7: $E^- + H = OH^- + H_2$	2.5E10
RE8: $E^- + H_2O_2 = OH + OH^- + H_2O$	1.3E10
RE9: $E^- + H_2O = H + OH^- + H_2O$	1.6E1
RE10: $H^+ + OH^- = H_2O$	1.43E11
RE11: $H_2O = OH^- + H^+$	2.599E-5
RE12: $2H = H_2$	8E9
RE13: $H + OH = H_2O$	2E10
RE14: $OH + H_2 = H + H_2O$	4.5E7
RE15: $OH + H_2O_2 = H_2O + HO_2$	2.3E7
RE16: $H + H_2O_2 = OH + H_2O$	9E7
RE17: $E^- + O_2 = O_2^- + H_2O$	1.9E10
RE18: $H + O_2 = HO_2$	1.9E10
RE19: $HO_2 = O_2^- + H^+$	8E5
RE20: $H^+ + O_2^- = HO_2$	5E10
RE21: $HO_2 + O_2^- = O_2 + HO_2^-$	7.9E7
RE22: $H + HO_2 = H_2O_2$	2.2E10
RE23: $H + O_2 = HO_2$	2E10
RE24: $E^- + HO_2 = HO_2^- + H_2O$	2E10
RE25: $E^- + O_2 = HO_2^- + OH^-$	1E10
RE26: $OH^- + H_2O_2 = HO_2^- + H_2O$	5E3
RE27: $H_2O + HO_2^- = H_2O_2 + OH^-$	5.735E-1
RE28: $O^- + O^- = O_2^{--}$	E9
RE29: $O^- + HO_2^- = OH^- + O_2^-$	4E8
RE30: $O_2^{--} + H_2O = HO_2^- + OH^-$	1
RE31: $O^- + H_2O = OH + OH^-$	2
RE32: $O^- + H_2 = OH^- + H$	8E7
RE33: $OH + OH^- = O^- + H_2O$	1.4E4
RE34: $O^- + E^- = 2OH^-$	2E10
RE35: $E^- + HO_2^- = O^- + OH^- + H_2O$	3.5E9

Table 3 continued

	<u>Rate constant</u> <u>M<sup>-1</sup> s<sup>-1</sup></u>
RE37:H <sub>2</sub> = Dummy 1	E4
RE39:O <sub>2</sub> = Dummy 2	E4
RE40:Dummy 1 = H <sub>2</sub>	62.9
RE41:Dummy 2 = O <sub>2</sub>	104
RE42:O <sub>2</sub> <sup>-</sup> + O <sub>2</sub> <sup>-</sup> = O <sub>2</sub> + O <sub>2</sub> <sup>--</sup>	E6
RE43:OH + O <sup>-</sup> = HO <sub>2</sub> <sup>-</sup>	1.8E10
RE44:OH + HO <sub>2</sub> <sup>-</sup> = H <sub>2</sub> O + O <sub>2</sub> <sup>-</sup>	7.5E9
RE45:O <sup>-</sup> + O <sub>2</sub> <sup>-</sup> = O <sub>3</sub> <sup>--</sup>	6E8
RE46:O <sup>-</sup> + H <sub>2</sub> O <sub>2</sub> = O <sub>2</sub> <sup>-</sup> + H <sub>2</sub> O	5E7
RE47:O <sub>3</sub> <sup>--</sup> + H <sub>2</sub> O = O <sub>2</sub> + 2OH <sup>-</sup>	1



TABLE 4. Additional reactions in the presence of iron ions,  $\text{NO}_2^-$  and  $\text{NO}_3^-$ 

	<u>Rate constant</u> <u><math>\text{M}^{-1} \text{s}^{-1}</math></u>
RE48: $\text{Fe}^{++} + \text{O}^- = \text{Fe}^{+++} + \text{O}^{--}$	3.4E8
RE49: $\text{Fe}^{++} + \text{OH}^- = \text{Fe}^{+++} + \text{OH}^-$	3.4E8
RE50: $\text{Fe}^{++} + \text{E}^- = \text{Fe}^{+++} + \text{OH}^- + \text{H}^-$	1.2E8
RE51: $\text{H}^- + \text{H}_2\text{O} = \text{H}_2 + \text{OH}^-$	E-2
RE52: $\text{Fe}^{++} + \text{HO}_2^- = \text{Fe}^{+++} + \text{OH}^- + \text{O}^-$	60
RE53: $\text{Fe}^{++} + \text{H}_2\text{O}_2 = \text{Fe}^{+++} + \text{OH}^- + \text{OH}^-$	60
RE54: $\text{Fe}^{++} + \text{H} = \text{Fe}^{+++} + \text{H}^-$	1.3E7
RE55: $\text{Fe}^{++} + \text{O}_2^- = \text{Fe}^{+++} + \text{O}_2^{--}$	4E8
RE56: $\text{Fe}^{+++} + \text{E}^- = \text{Fe}^{++} + \text{H}_2\text{O}$	2E10
RE57: $\text{Fe}^{+++} + \text{O}_2^- = \text{Fe}^{++} + \text{O}_2$	4E8
RE58: $\text{Fe}^{+++} + \text{H} = \text{Fe}^{++} + \text{H}^+$	E8
RE59: $\text{O}^{--} + \text{H}_2\text{O} = 2\text{OH}^-$	E-2
RE60: $\text{O}^- + \text{NO}_2^- = \text{NO}_2 + \text{O}^{--}$	2.4E8
RE61: $\text{OH}^- + \text{NO}_2^- = \text{NO}_2 + \text{OH}^-$	2.4E8
RE62: $\text{E}^- + \text{NO}_3^- = \text{NO}_2 + 2\text{OH}^-$	9.5E9
RE63: $\text{H} + \text{NO}_3^- = \text{NO}_2 + \text{OH}^-$	E7
RE64: $\text{H} + \text{NO}_2^- = \text{NO} + \text{OH}^-$	E9
RE65: $\text{NO} + \text{NO}_2 = \text{N}_2\text{O}_3$	E2
RE66: $\text{N}_2\text{O}_3 + \text{H}_2\text{O} = 2\text{H}^+ + 2\text{NO}_2^-$	E-2
RE67: $\text{NO}_2 + \text{NO}_2 = \text{N}_2\text{O}_4$	E2
RE68: $\text{N}_2\text{O}_4 + \text{H}_2\text{O} = 2\text{H}^+ + \text{NO}_3^- + \text{NO}_2^-$	E-2

TABLE 5. Production of hydrogen and oxygen in cemented cladding hull waste in a thin alpha irradiated water layer

Time period Y	H <sub>2</sub> mol/y	G-value	O <sub>2</sub> mol/y	G-value	Integrated gas product. l at 0°C, 0.1MPa
3-40	0.427	1.05	0.213	0.52	530
40-100	0.376	1.05	0.188	0.52	1290
100-10 <sup>3</sup>	0.212	1.04	0.106	0.52	7700
10 <sup>3</sup> -10 <sup>4</sup>	0.0611	1.04	0.03055	0.52	26000
10 <sup>4</sup> -10 <sup>5</sup>	0.0113	0.91	0.00565	0.45	60000

TABLE 6a. Production of hydrogen in the free water phase of cemented cladding hull waste. Hydrogen is assumed to disappear by diffusion through a bentonite layer. The water is assumed to be initially deaerated.

Storage period, y	Mean dose rate rad/s	Equilibrium concentr in liquid phase μM		G(H <sub>2</sub> )	Prod(H <sub>2</sub> ) mol/y	Integrated hydrogen production l (STP)
		H <sub>2</sub>	O <sub>2</sub>			
3-40	5.5	0.44	0.13	1.09E-7	4.4E-6	2.6E-3
40-100	2.1	0.46	0.18	3.2E-7	4.0E-6	8E-3
100-1000	1.13	0.51	0.25	5.7E-7	4.0E-6	8.9E-2
10 <sup>3</sup> -10 <sup>4</sup>	0.32	0.43	0.21	1.68E-6	3.4E-6	0.77
10 <sup>4</sup> -10 <sup>5</sup>	0.77	0.35	0.17	5.7E-6	2.7E-6	6.2

TABLE 6b. Production of hydrogen in the free water phase of cemented cladding hull waste. Hydrogen is assumed to disappear by diffusion through a bentonite layer. The water is assumed to be initially aerated at 0.1 MPa

Storage period, y	Mean dose rate rad/s	Equil. conc. mM, H <sub>2</sub> <sup>-</sup>	G(H <sub>2</sub> )	Prod(H <sub>2</sub> ) mol/y	Integrated H <sub>2</sub> prod. l (STP)
3-40	5.5	0.235	8.9E-5	3.04E-3	2.5
40-100	2.1	0.248	1.53E-4	2.01E-3	5.2
100-10 <sup>3</sup>	1.13	0.248	2.78E-4	1.94E-3	44.7
10 <sup>3</sup> -10 <sup>4</sup>	0.32	0.250	9.81E-4	1.96E-3	4.38
10 <sup>4</sup> -10 <sup>5</sup>	0.077	0.244	4.00E-3	1.90E-3	4265

TABLE 6c. Production of hydrogen in the free water phase of cemented cladding hull waste. Hydrogen is assumed to disappear by diffusion through a water layer. The water is assumed to be initially aerated at 0.1 MPa.

Storage period, y	Mean dose rate rad/s	Equil. conc. mM, H <sub>2</sub>	G(H <sub>2</sub> )	Prod(H <sub>2</sub> ) mol/y	Integrated H <sub>2</sub> prod m <sup>3</sup> (STP)
3-40	5.5	0.234	3.58E-2	1.22	1.0
40-100	2.1	0.218	8.59E-2	1.13	2.5
100-10 <sup>3</sup>	1.13	0.191	1.38E-1	0.970	22
10 <sup>3</sup> -10 <sup>4</sup>	0.32	0.099	2.65E-1	0.527	128
10 <sup>4</sup> -10 <sup>5</sup>	0.077	0.035	4.00E-1	0.190	510

TABLE 7. Production of hydrogen in cemented cladding hull waste.  
Assumption: 190 l free water in contact with 100 l gas phase

Storage period, y	Mean dose rate rad/s	Equilibrium concentration in liquid phase		Equilibrium pressure, MPa		Total pressure MPa
		$\mu\text{M}$				
		H <sub>2</sub>	O <sub>2</sub>	H <sub>2</sub>	O <sub>2</sub>	
3-40	5.5	1.02	0.80	1.3E-4	6E-5	Deaerated conditions
40-100	2.1	0.94	0.74	1.2E-4	6E-5	
3-40	5.5	1070	1090	0.14	0.07	0.2 Aerated*
40-100	2.1	1370	1340	0.18	0.09	0.26 conditions

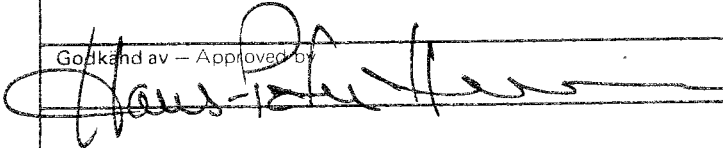
\* The given values are a little below equilibrium values

TABLE 8. Gamma-radiolysis of concrete at a pH of 12.3  
using varying dose rates (see text, case 1)

Dose rate rad/s	Final gas Pressure		Irradiation time s	
	MPa	psig		
	3.890	0.25		
389	0.24	34	1.3E7	
39	0.24	34	1.1E8	

APPENDIX 1

**Studsvik Arbetsrapport** - Technical Report

Projektidentifikation -- Project identification	Datum -- Date 830125	Org enh och nr -- Report No. NW-83/416
Titel och författare -- Title and author ELECTRONS TRAPPED IN CRYSTALLINE SYSTEMS CONTAINING WATER  Z P Zagórski Department of Radiation Chemistry Institute of Nuclear Research Warsaw, Polen		
Distribution		
Godkänd av -- Approved by 	Kontonr -- Internal notes PN4956A	<input type="checkbox"/> Rapporten skall förhandsviseras
<p style="text-align: center;">INTRODUCTION</p> <p>The majority of work on electrons at low temperatures has been done on glass systems. One of the reasons for this is without any doubt the simplicity of experimental approach. The easiest method of studying trapped electron is to deal with its characteristic and intense absorption spectrum. The glass matrix makes the task comparatively easy. There is, of course the deeper motivation for the glass system. Such a matrix is well motivated as the object of study by its direct relation to the liquid systems. Like in liquids, one can add a diversity of additives, and have a homogenous and transparent but rigid system of high viscosity with elements of the structure practically immobilized.</p> <p>However, the fact of life is, that the majority of solid aqueous systems, at any temperature, is of crystalline structure, usually more stable than the glassy one. Electrons are easily stabilized in crystalline material; in a variety of ways the <math>e_t</math> chemistry seems to be even richer and more interesting than it is in glass systems.</p>		

The experimental approach is much more difficult and the present paper gives only a few facts in the hope that the radiation chemistry of electrons in crystalline material will eventually reach the level corresponding to  $e_t^-$  in glass materials.

#### General survey of the irradiated matrix

The matrix treated in the present paper is limited to alkaline-aqueous systems. It comprises not only Na and K hydroxides but takes into account tetralkylammonium hydroxides which behave in many respects similar, thus helping to eliminate the role of cations.

Figure 1 shows the field of research; the variety of systems at different temperatures. It is obvious that the glassy state is rather an exceptional, rigid state of undercooled liquid, thus thermodynamically unstable. It changes easily into polycrystalline state. Limits of concentration of hydroxides in which glass is formed are well defined: there is no possibility to obtain a glassy state below 6 mole KOH (NaOH) per liter. The limited solubility of  $R_4NOH$  in water probably prevents the preparation of glass at all. There is no possibility to obtain mixed,  $Na^+$ ,  $K^+$ ,  $R_4N^+$  hydroxides in the glassy state, because of salting-out effect.

#### Glassy versus crystalline state

A popular criterion of the glassy state is the transparency of the frozen sample. In the case of sodium and potassium hydroxides that criterion is true but it fails in the case of tetrabutylammonium hydroxide - clathrate, not to mention solid ammonia and other systems.

Looking for a deeper understanding of the differences between crystalline and glassy states, we have determined systematically the density of KOH and NaOH solution at 77 K. Results show a marked difference between the two states (Fig 2). The glassy state is substantially more dense, i e more tightly packed than the crystalline or polycrystalline preparation. The average distance between molecules and ions is significantly shorter in glasses. The difference is substantial indeed: Taking the NaOH solution of starting concentration of 6.2 mole/l at room temperature, the crystalline material has a density of 1.19 g/ml (77 K) whereas the corresponding glassy material has 1.28 g/ml (77 K). Or, if we consider the density 1.19 g/ml, it corresponds to 3.8 mole/l (hypothetical) glassy material, or 6.2 mole/l - polycrystalline material.

Still more examples may be found in the high concentration zone.

In view of the drastic differences in density, it would be reasonable to refer to the real volume when describing the concentration. E g the glass obtained from 12 mole/l NaOH solution, att 77 K is really 12.3 mole/l. Correspondingly, the solid  $\text{NaOH} \cdot \text{H}_2\text{O}$  has the molarity of 29.8 mole/l at room temperature or 29.6 at 77 K.

The differences of densities have a practical aspect in the experimental technique. Glass is prepared easily because substantial contraction does not introduce any mechanical forces. However, the freezing of 0-5 M solutions or slow freezing of a concentrated solution (e g 12 M at -138 K) invariably destroys all vessels by

forceful expansion. Also the slow rewarming of glass systems, connected with the formation of an expanded crystalline phase, destroys the vessel.

The determination of density also learns that a rapidly cooled polycrystalline material has a pretty regular composition. The glassy material obtained by rapid cooling of concentrated solutions (at the same rate of cooling), is no longer as regular. We can conclude that polycrystalline material does not contain a heavy packed glassy fraction, but in glassy material some crystalline, light fraction may be present. That applies specially to KOH solutions (cf Fig 2b). Figures 2a and 2b were originally published in 1979 /1/, but since that time enriched with more points, especially describing crystalline preparations of high sodium hydroxide concentration.

#### Methods of polycrystalline matrix investigations

Before describing experiments on electrons trapped in a polycrystalline matrix, one has to do as much as possible about the recognition of the matrix itself.

The knowledge of this sort of matrix is rather poor and the solid state chemistry does not contribute very much in this respect. Our systems are outside the traditional interests of solid state chemistry, which is, still traditionally limited to silicates as concern glassy material and to cases of crystalline materials of applied interest, like semiconductors. Very seldom hydroxides, nitrates, hydrates etc are investigated.



Especially solid hydrates, which are the main object of our investigation, a favourable matrix for electron traps, are poorly known. Except for a few celebrated cases like  $\text{LiClO}_4 \cdot 3\text{H}_2\text{O}$ ,  $\text{BeSO}_4 \cdot 4\text{H}_2\text{O}$ ,  $\text{CuSO}_4 \cdot 5\text{H}_2\text{O}$  and others, the knowledge is not deep. The knowledge is specially insufficient in the case of hydrates which trap electrons with special efficiency.

For instance, there is only one paper written in the recent two decades on the system water-sodium hydroxide /2/ describing the existence of several hydrates and one study on  $\text{NaOH} \cdot 4\text{H}_2\text{O}$  structure. There is no information on KOH.

The most important is X-ray analysis but the majority of equipment does not accept hygroscopic and caustic samples and low temperature work. Only few measurements were performed in the Institute of Physical Chemistry in Warsaw, were X-ray diffraction patterns confirmed our conclusions (see the paragraph about density) that the glassy material contains varying amounts of crystalline centers.

There are other simple experimental approaches possible, which contribute to the knowledge of the matrix. We have applied thermogravimetric and differential thermoanalysis which earlier proved its value in the investigation of hydrates. Indeed, that method helped us to formulate the composition of  $\text{KOH} \cdot 1/2\text{H}_2\text{O}$ , to decide if all the water in a hydrate containing more than one molecule of water, is equally coordinated.

Looking for a specific behaviour of some hydrates, we have also applied IR spectrophotometry. The reason was the distinct behaviour of hydrates obtained from alkaline solutions:

$\text{NaOH}\cdot\text{H}_2\text{O}$ ,  $\text{K}_3\text{PO}_4\cdot 3\text{H}_2\text{O}$ ,  $\text{Na}_2\text{HPO}_4\cdot 2\text{H}_2\text{O}$  (but not  $\text{NaH}_2\text{PO}_4\cdot\text{H}_2\text{O}$ ),  $\text{Na}_2\text{CO}_3\cdot\text{H}_2\text{O}$ ,  $\text{Na}_2\text{SO}_3\cdot 7\text{H}_2\text{O}$ ,  $2\text{K}_2\text{CO}_3\cdot 3\text{H}_2\text{O}$ ,  $\text{LiOH}\cdot\text{H}_2\text{O}$ ,  $\text{Ba}(\text{OH})_2\cdot 8\text{H}_2\text{O}$ ,  $(\text{CH}_3)_4\text{NOH}\cdot 5\text{H}_2\text{O}$ ,  $\text{BaCl}_2\cdot 2\text{H}_2\text{O}$ .

Finally some methods had to be applied, which say something about the homogeneity and texture of polycrystalline materials. These methods are not necessary in the case of glassy systems, where one believes, probably with justification, that the system is ideally disordered and that every additive is distributed with a perfect homogeneity.

It may not be the case with polycrystalline material. During the crystallization the process of fractionation takes place. However, a rapid cooling secures at least a macro-homogeneous composition.

Experimental investigation of electrons trapped in polycrystalline material at low temperatures.

Polycrystalline material is usually opaque, from semitransparent, slowly frozen  $<6$  mole/l solutions, to more opaque, cooled melts of hydrates, to practically white pigmentlike 10 mole/l NaOH solutions frozen first under mixing at 135 K and later cooled to 77 K. Even semitransparent preparations can not be investigated spectrophotometrically because the extinction at 1 mm thickness, already without trapped electrons, exceeds 3. The reflective spectrometry is vaguely mentioned, but no results has been published yet.

The pulse radiolysis method using the Cherenkov light selfabsorption brought the solution to the problem of detection of intermediates in opaque media. The method helped to investigate the phenomenon of trapped electrons in a matrix of very low water content (e g  $\text{KOH} \cdot 1/4\text{H}_2\text{O}$ ) and to formulate the thesis of "one water molecule-one electron" responsible for the electronic spectrum /3/.

Our Cherenkov Light Selfabsorption Method is useful in measurements also at low temperatures. It is a little more complicated than at room temperature but a proper vessel makes the task comparatively easy. The opaqueness of the sample slows down the process of bleaching, if such is needed. For that purpose we are using light with the maximum of intensity shifted to IR. The increase of the local temperature and higher penetration of IR in the matrix of many internal reflections speeds up the bleaching. Such a procedure would not have been acceptable in the case of glass, where local warming could produce annealing phenomena. With the polycrystalline material no structural changes are expected, and only desired ones, i e the emptying of traps, is achieved.

The second method used in the investigation of electrons at low temperatures in polycrystalline material consists in collection of the charge, released later during the illumination of previously irradiated samples /4/.

## RESULTS

The unconventional method of pulse radiolysis using the Cherenkov Light Selfabsorption may rise doubts concerning its veracity. Therefore we have applied it to the transparent system which may be investigated by both spectrophotometric methods, using external or internal analyzing light. The system chosen was electrons trapped in glassy NaOH solution, 10 mole/l. Figure 3 shows that the maximum of absorption measured by both methods is the same. The Cherenkov Method gives more information i.e. the spectra at the beginning of the pulse is the same. The slight difference at the red part of the spectrum cannot be explained until IR measurements will be done. They are very difficult due to the low level of Cherenkov light in the red region. Experiments on monocrystals by conventional pulse radiolysis are also planned.

The polycrystalline systems investigated by pulse radiolysis at low temperatures were hydroxides of sodium, potassium and tetraalkylammonium cations. Spectra are very similar and small shifts of maxima can hardly be attributed to the cation, but there are blue shifts of the spectrum with diminishing contents of water /5, 6/.

At a very low content of water (e.g. KOH.1/4H<sub>2</sub>O) in the matrix only the blue shift is observed, but the difference between room temperature and 77 K is not a marked one. The interaction of electron with one molecule of water is decisive and the influence of the matrix is slightly more pronounced in comparison with the mainly aqueous system (Fig 4).

Figure 5 shows the estimated kinetics of the  $e_t^-$  decay, extrapolated from calculations of the build-up curve. That curve results from the linear formation and exponential decay of  $e_t^-$ . The algorithm is similar to the case of activation by the neutron beam of a nuclide which decays rapidly.

The question is very often asked about the  $e_t^-$  spectrum in KOH or NaOH free from water. With the disappearance of the last traces of water also the characteristic spectrum disappears. One observes a very faint spectrum (Fig 6) with the maximum at ca 400 nm which does not disappear in microseconds at room temperature, but is permanent like F centers in irradiated halogenides (e g KCl).

Final conclusions are hoped to be reached after the completion of esr investigations, which have just started, of the X-ray and neutronographic ones due to begin, and analysis of products, especially important in the case of  $R_4NOH \cdot nH_2O$ .

Another question asked is that of the final stable products. Already the pulse radiolysis work shows that the production of stable new compounds is rather low. Subsequent pulses applied to the same sample after the time needed for recording of the kinetic curve give the same result. That indicates either the formation of products of radiolysis which do not take part in the stabilization of electrons or the yield of radiolysis calculated as permanent radiation damage is negligible. We were looking for the presence of hydrogen by gas chromatography and for hydrogen peroxide by polarography, after the dose of 10 Mrads applied carefully without an

increase of temperature higher than is the case during pulse radiolysis work. No products of radiolysis could be found.

As experiments performed at extreme temperatures (room temperature and liquid nitrogen) give different results as concerns the stability of the trapped electron, we have made an attempt to look into phenomena at intermediate temperatures. Such an approach was necessary also because of the necessity to compare results with only two papers dealing with radiation chemistry of sodium hydroxide hydrates, low water, crystalline, but at liquid nitrogen temperature. Our experiment was difficult, because of the slow adjustment of a precise intermediate temperature. One can make a vague statement that around  $-50^{\circ}\text{C}$  a rather stable trapping occurs, but if that temperature has the character of a threshold remains an open question. However, already at that temperature a distinct difference between the first and subsequent pulses is observed. The first pulse produces the familiar kinetic curve of build-up of the trapped electron spectrum. Next pulses applied to the same sample produce only constant Cherenkov emission without the usual selfabsorption. That indicates a saturation of existing traps.

#### Irradiation of concrete

After 10 years of operation of our linear electron accelerator, we have realized, that below the processing window, the concrete received the dose of ca 1 Trad (10GGy) of electrons (10-13 MeV). The place was always covered with a thin sheet of aluminium, thus being not spoiled by dirt and graphite etc from the conveyor. The temperature at that place reached sometimes up to  $100^{\circ}\text{C}$  (empty conveyor).

Except of a light reddish colour, the concrete did not show a dramatically diminished resistance, indicating dissipation of ionizing energy into heat with negligible chemical effect.

To examine the phenomenon more closely, samples of Portland cement SP 550 of Polish production (Cement Works Goraźdże - Danish Licence) were hydrated for 30 days at room temperature, and later, after drying, were irradiated under controlled conditions with the same machine, but this time using the polyenergetic straight beam of electrons. The sample was placed 17 cm from the window. The diameter of the beam (half-gaussian) was 18 mm. At the centre of the sample, a thermoelement was placed (Sodern Thermocoax, Chromel Alumel 2AB Ac o5, Gaine Inox diam 0.5 mm) of the sort used in reactor technique, extremely resistant to ionizing radiation. The sample was intensively cooled by air. The flux of energy was adjusted at such a level that the temperature did not reach a zone higher than 108-116<sup>o</sup>C. These were the limits in which the equilibrium oscillated, between the supplied energy and the heat taken by air. Thus the maximum dose rate was reached, ca 2000 Mrad/h. The sample looked unchanged, except small cracks (the cement was hydrated without sand). It did not change colour like our old sample. The last one probably contained much iron.

More experiments are planned on irradiated samples, especially thermogravimetric and thermoanalytical ones.

## DISCUSSION

Several aspects of the investigated system have to be considered if a reasonable understanding of the phenomena is the aim of our research. The first thing is a clear differentiation between the liquid, solid-glassy and the solid-poly-crystalline states from the point of view of radiation chemistry. Early phenomena are slightly influenced by the state of the system, but if we move deeper in the time scale, the influence of the structure, and later even of the texture of the system is more and more pronounced.

Figure 7 shows the space-time development of small isolated energy deposit (spur) in a diluted aqueous system, slightly modified, or rather edited from the recent paper by Magee and Chatterjee (7). Although some points in that scheme are still controversial, the picture is generally accepted. The next Figure 8 shows in the same ordinates phenomena in a chemically similar but rigid system. The impossibility for intermediates to diffuse as quickly as in the solution is obvious. Less obvious is the difference in the dielectric relaxation. Here we are touching an old question, raised already in the fifties, before the discovery of the hydrated electron: How far may an electron travel from the parent positive ion. The critical radius, called the Onsagers radius, depends on the dielectric constant of the medium. The classical textbook calculations says, that in polar liquids like water ( $\epsilon \approx 80$ ) the critical distance is only 0.7 nm at 300 K, whereas in nonpolar liquids (e.g. liquid hydrocarbons) the distance is ca 28 nm. Looking into rigid systems containing water, are we allowed to draw the same conclusions?



If so, the travelling distance of the electron here is always rather long because the dielectric constant (the high frequency one, the same as accepted for liquid water) is low both in solid hydrates and in ice. The dielectric constants for the hydrates we are mainly investigating are not available, but similar ones have low values:  $\text{Na}_2\text{CO}_3 \cdot 10\text{H}_2\text{O}$  - 5.3 (anhydrous has even 8.4!),  $\text{BaCl}_2 \cdot 2\text{H}_2\text{O}$  has 9.4 (anhydrous has even 11.4), all values for frequency  $6 \times 10^7$  Hz, etc, etc (according to /8/). The same source does not quote values for ice, but in monographs on water /9,10,11/ we can find low values. In one of the handbooks /12/ we found  $\epsilon = 69.4$  at  $-10^\circ\text{C}$  falling sharply down to 3.8 at  $-50^\circ\text{C}$ . In spite of the enormous work done on frozen glassy systems, we were not able to find data on dielectric constants of alkaline glasses.

Nevertheless, a low dielectric constant in frozen aqueous systems and of hydrates at all temperatures, seems to be a general fact and may be used in the discussion.

What really matters is not the dielectric constant itself, but a proper estimate of the kinetics of relaxation of water molecules. Looking for that, Kevan /13/ has calculated, that if the temperature is decreased from 260 K to 77 K the duration of the dielectric relaxation in water ice, is increased from  $6.4 \times 10^{-5}$  to  $10^{22}$  s. It means that in the range of 130-110 K water dipoles are already practically motionless and fixed. The obvious next conclusion is that the electron is trapped in existing defects of the lattice. The presence of ready electron traps is suggested also by Taub and Eiben /14/.

The very large differences in density between systems in the glassy and polycrystalline states drew our attention to interpret them in terms of internal energy. Sodium (or potassium) hydroxide solutions of concentrations higher than 6 M mentioned in "Results" are well suited for this sort of consideration, because their chemical summary composition is the same, but structural differences are reflected in a different density of packing. The glassy variety is meta-stable and is relaxing to the polycrystalline form of more loose structure and higher volume. Lower density manifests itself sometimes in a very dramatic mode, causing a violent destruction of the vessel with frozen glass, if the heating is slow, and the system has time to rearrange into crystals before melting.

The investigation of the glassy vs. the polycrystalline system from the point of view of thermodynamics has just started. We are trying to make as much use from the rather precisely measured difference in density. Other measurements would be necessary to have a full picture: the heat of change from glassy into crystalline form, the temperature coefficient of density around 77 K,  $\alpha_p = \left( \frac{\partial \ln V}{\partial T} \right)_p$  as well as the influence of pressure on the density at constant temperature. The first characteristics seems simple enough to realize from the Hess cycle: what is needed is only the dissolution of glassy and in the next experiment the crystalline sample in the water calorimeter, both samples of the same weight and frozen to the same temperature of 77 K. We did not succeed yet in making that experiment with a satisfactory precision. The same applies to the measurement of the temperature coefficient of density. There is little choice of liquefied gases with boiling temperature close to that of

liquid nitrogen. The third value (that of the dependence of the density on pressure, practically impossible to measure, may be neglected, because it is of little influence on the result.

We may safely accept, that the transformation from glassy state into crystalline ( $\alpha \rightarrow \beta$ ) is not connected with any chemical changes, with any changes of the hydration of ions involved (sodium and hydroxide) and of their interaction with the medium. If so, we may consider a change from a densely packed system of randomly arranged molecules of hydration into a more loosely packed system of similar molecules of hydration, this time rearranged and regularly filling the space. Both systems may be characterized by distinctly different potential energy curves. Now the difference of internal energy may be described as

$$\beta_{\Delta} \alpha H = \int_{\rho\alpha}^{\rho\beta} \left( v - T \left( \frac{\partial v}{\partial T} \right)_p \left( \frac{\partial p}{\partial \rho} \right)_T \right) d\rho$$

$$\beta_{\Delta} \alpha H = \int \left( T \left( \frac{\partial \ln v}{\partial T} \right)_p - 1 \right) \frac{1 \text{ kg}}{\rho} \left( \frac{\partial p}{\partial \ln v} \right)_T \frac{d\rho}{\rho}$$

After several simplifications substituting the lack of experimental data one obtains for  $\beta_{\Delta} \alpha H$  value  $-560 \text{ kJ/kg}$ , or  $-135 \text{ kcal/kg}$ . At this stage of research it would not be reasonable to make further conclusions. However, operating with order of magnitudes one can state that the indicated energy recalculated on 1 mole of water is equivalent to the energy of 1 mole of hydrogen bonding. Even another comparison is possible: The enthalpy of transformation  $\alpha \rightarrow \beta$  recalculated into 1 mole of water equals approximately one third of the enthalpy of evaporation at  $100^{\circ}\text{C}$ .

What consequences may be expected from the differences in internal energy of glassy and crystalline systems? It may be certainly noted that the radiation chemistry of glassy systems may be closer to liquid water than to ice.

Many interesting questions appear: May the local heating by the deposition of radiation energy cause local crystallization and release of new amounts of energy? Has the extra amount of energy in the shape of compressed matter something to do with the phenomenon of tunneling?

It is time now to arrive at some proposals of models on what is going on in crystalline, low water content systems, irradiated with almost any dose rate and total dose at room temperature. Proposing a mechanism we are in a much more difficult position in comparison to our colleagues working with systems more rich in water. Without any doubt the chief obstacle in the application of one of the models developed for the last mentioned systems is the most meager presence of water, not sufficient to secure the minimum of 4 water molecules around the electron to produce something like  $e_{aq}^-$ . We are able to eliminate some concepts from further consideration. For instance we may reject the concept of cation-electron pair, because of our most convincing experiment: introduction of tetraalkylammonium cation for sodium or potassium the picture of phenomena is the same - the electron does not "see" the cation at all. It would have been most difficult to imagine identity of the  $Na^+e^-$  pair and the  $NR_4^+e^-$  pair - of completely different size and mode of hydration. The idea of electron-cation pairs has been rejected also by Kevan in 1981 /15/: "Even though there is a very large

concentration of sodium ions (10 M), the electron spin-echo results show that the solvated electron has only water molecules in its first solvation shell". In spite of that the idea of ion pairs is very persistent, especially in Russian papers.

#### CONCLUSIONS

As it is a normal case in radiation chemistry and chemistry in general, the facts are clear reproduceable observed with reasonable precision and satisfaction, but their explanation is very obscure. I have spent quite a time looking for inspiration in cold glass radiation chemistry, which in two cases (Report by Wieczorek, /16/ and a paper by Puntezhis, Ershov and Pikaev /17/) was trying to investigate well defined sodium hydroxide hydrates, unfortunately not going below 2 molecules of water per 1 of NaOH.

However, even the aqueous glass radiation chemistry is in confusion, concerning the origin of traps, their depth, kinetics of trapping and of the release, reactions of holes, bleaching etc. Considerations of phenomena described by the dielectric constant at different frequencies, which were giving rather good results, being a right guide in the liquid state of different polarity, here, i e in the solid state, seem to be meaningless. Kieffer /18/ writes in his recent (1981) NATO lecture: "The case of electron solvation in ice is particularly interesting in that it occurs on a time-scale which is completely incompatible with the dielectric relaxation time of the medium". I did not even touch the question of tunneling, popular in low temperature glasses

but not clear as concerns the mechanism. In crystalline hydrates research no tunneling was observed yet.

Let us make some speculations on the radiation chemistry of crystalline hydrates irradiated at room temperature. A look at Magees scheme (Fig 7) will help to find out some real differences. The first energy deposit is probably not affected by the particular state of the condensed phase, the high energy radiation does not see the movement of molecules. Consequently, the spurs are of the same structure as in any condensed phase. As usual, the degradation of energy results in closer and closer ionization sites and in the inevitable occurrence of several ionizations very close to themselves in a small volume located in the unchanged bulk of the medium. Therefore, also in the solid state, the classical diagram by Mozumder and Magee /19/ is valid here describing the percentage contribution of spurs, short tracks and blobs, according to the energy of primary electrons. Quantum mechanical treatment of low energy electrons is also valid here. The length of the De Broglie wave ( $\lambda = h/mv$ ) is for a 100 eV electron 0.1 nm, for 1 eV 1.2 nm, for 0.1 eV ca 4 nm and for thermal energies a 7 nm. Unfortunately there is nothing known yet about infrared electrons in crystalline hydrates (the experiment is still in preparation due to many difficulties).

If there is no doubt about the same spur distribution in liquid and glassy solid states, so there may be some questions whether the crystalline state may influence the early deposition of energy. There are some indications that the reactive intermediates may migrate in the

crystal to its surface. Another question is the role of defects more or less specific to hydrates. Practically nothing is known, and there may be only our guess about that. Another justified guess is the presence of phonons, without any doubt very active at room temperature in the annealing of radiation induced changes.

At present I am trying to formulate the following picture of events in hydrates of low water content: Electrons released in the ionization process and almost thermalized are trapped by one molecule of water. It is practically only Hamill who postulated the formation of  $\text{H}_2\text{O}^-$  /20/. My argument for that species is purely a geometrical one: I cannot imagine the formation of the usual  $e_{\text{aq}}^-$  with four or six water molecules in  $\text{KOH} \cdot 1/4\text{H}_2\text{O}$ . Indeed, moving to higher hydrates the spectrum comes more and more close to classical  $e_{\text{aq}}^-$ . Nevertheless the majority of radiation chemists rejects the  $\text{H}_2\text{O}^-$  idea. If really that idea is theoretically indigestible, I can propose as an alternative the trapping of the electron in the  $\text{OH}^-$  vacancy close to the water molecule. That concept may be supported by the higher oscillator strength of the spectrum in hydrated hydroxides or hydrates in which  $\text{OH}^-$  ions may be present and by the effect of saturation of traps occurring already at ca  $-50^\circ\text{C}$ .

The positive hole has to be identified as  $\text{H}_2\text{O}^+$ , but its fate is as mysterious as the electron trap. There are all indications that  $\text{H}_2\text{O}^+$  does not react with the neighbouring water molecule, or the participation of that reaction, called by Magee in the case of liquid aqueous solutions as the fastest reaction in radiation chemistry, is

negligible. Otherwise the total degree of radiolysis would have been larger. We have to accept, that  $H_2O^+$  is waiting for an electron, released after a short sojourn from the trap. The  $e_m^-$  is of lower than initially energy so that the excited water formed in the reaction with  $H_2O^+$  does not produce an overexcited water molecule, able to dissociate into radicals; instead, it becomes thermalized without any chemical effect.

In low water hydrates,  $H_2O$  constitutes only as a part of the system and the rest, usually the main constituents, is of a quite different composition. Some sort of radiolysis goes on parallel to radiolysis in the aqueous part of the system and also with no chemical result. The intermediates in the nonaqueous part do not manifest themselves in pulse radiolysis because of lack of optical absorption or a low  $\epsilon$ . The situation may change in the case of organic cations or a neutral compound in the case of organic hydrates. Literature data show /21/ that penicillin trihydrate undergoes very low decomposition during radiation sterilization. The phenomena are similar to that described above, but one can assume vaguely that a part of the energy is taken by the aqueous part of the system thus acting as some sort of energy sink.

The continuing research is hoped to bring new facts which may confirm or totally change the presented picture.



## REFERENCES

- /1/ ZAGÓRSKI Z P, GRODKOWSKI J  
Nukleonika 24, 965 (1979).
- /2/ COHEN-ADAD R, TRANQUARD A, PÉRONNE R,  
NEGRI P AND ROLLET A P  
C. Rendus 1960, 2035.
- /3/ ZAGÓRSKI Z P  
Nukleonika 22, 725 (1977).
- /4/ GRODKOWSKI J, ZAGÓRSKI Z P  
Nukleonika 24, 867 (1979).
- /5/ ZAGÓRSKI Z P, BOBROWSKI K, GRODKOWSKI J  
Chem. Phys. Letters 59, 533 (1978).
- /6/ ZAGÓRSKI Z P, GRODKOWSKI J, BOBROWSKI K  
Radiat. Phys. Chem. 15, 343 (1980).
- /7/ MAGEE J L AND CHATTERJEE A  
LBL-9078, Berkeley 1979.
- /8/ Handbook of Chemistry and Physics,  
56th Ed., CRC Press, Cleveland, Ohio  
1976.
- /9/ EISENBERG D AND KAUFMANN W  
"The Structure and Properties of  
Water", Oxford at the Clarendon Press,  
1969.
- /10/ HORNE R A (editor)  
"Water and Aqueous Solutions", John  
Wiley, New York, 1972.
- /11/ FRANKS F (editor)  
"Water a Comprehensive Treatise",  
Plenum Press, New York, London 1973-1979,  
6 Volumes.
- /12/ "Spravochnik Khimika", 7 Volumes, Izd.  
"Khimiya", Leningrade 1968.
- /13/ KEVAN L  
Radiation Chemistry of Aqueous Systems,  
G. Stein (editor), Interscience Publishers,  
London 1968, 21 and in Action Chimiques  
et Biologiques des Radiations, M.  
Haissinsky (editor), Masson, Paris  
1969, Vol 13, 57.
- /14/ TAUB I A, EIBEN K  
J. Chem. Phys. 49, 2499 (1968).

- /15/ KEVAN L  
Accounts of Chemical Research 14, 138  
(1981).
- /16/ WIECZOREK H  
KFK 1717, Karlsruhe 1972.
- /17/ PUNTEZHIS S A, ERSHOV B G, PIKAEV A K  
Khim. Vys. Energ. 6, 153 (1972).
- /18/ KIEFFER F  
"The study of fast processes and  
transient species by electron pulse  
radiolysis" (Proc NATO Adv. Study  
Institute, Capri 1981), D. Reidel,  
Dordrecht 1982, p. 363-397.
- /19/ MOZUMDER A AND MAGEE J L  
Radiat. Res. 28, 203 (1966).
- /20/ RAZEM D, HAMILL W H  
J. Phys. Chem. 81, 1625 (1977).
- /21/ JACOBS G P  
Int. J. Appl. Radiat. Isotopes 30, 417  
(1979).

Figure 1

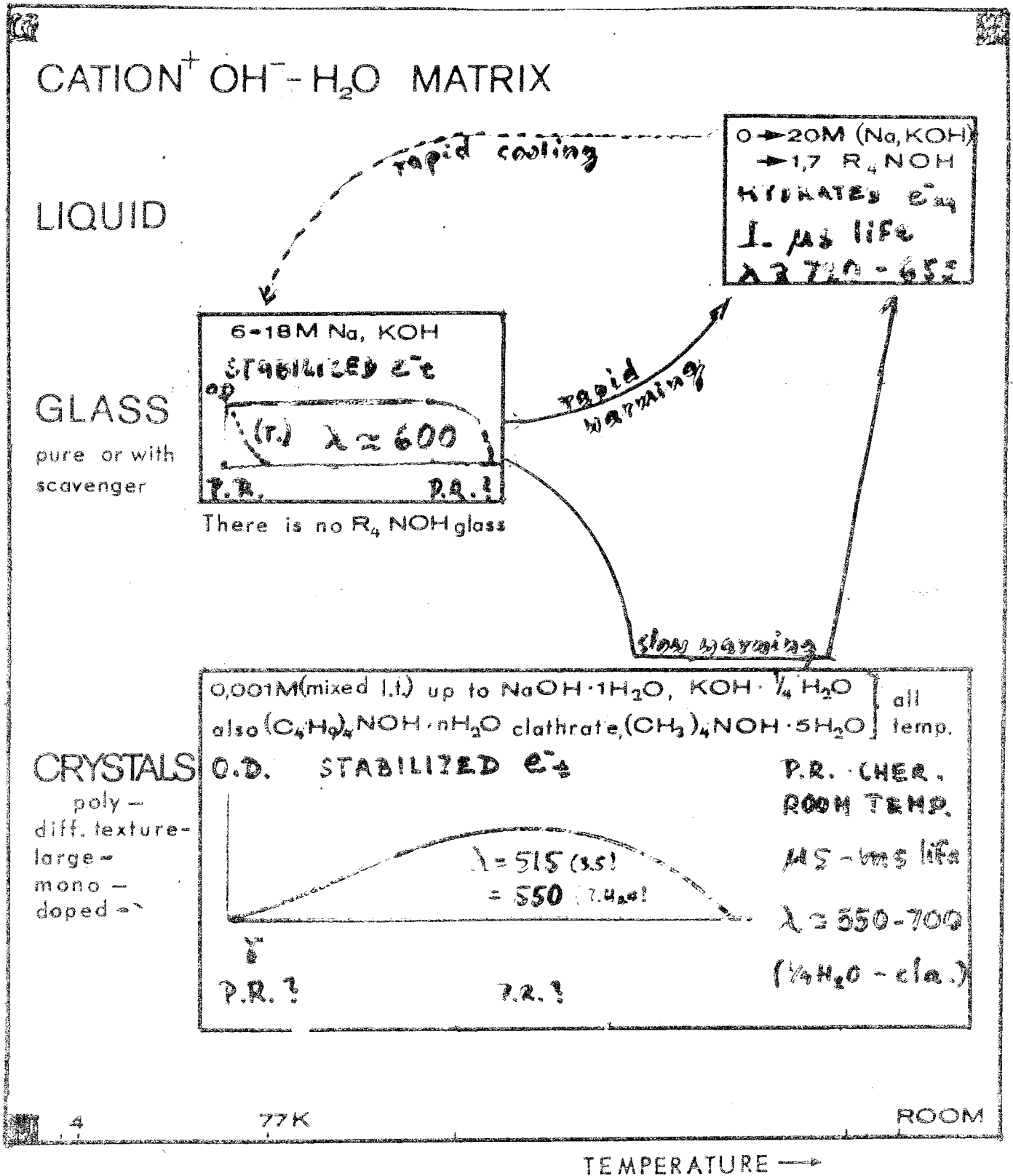


Figure 1. Types of motions in the cation<sup>+</sup> OH<sup>-</sup> H<sub>2</sub>O system and behaviour of trapped electron.

Figure 2a+2b

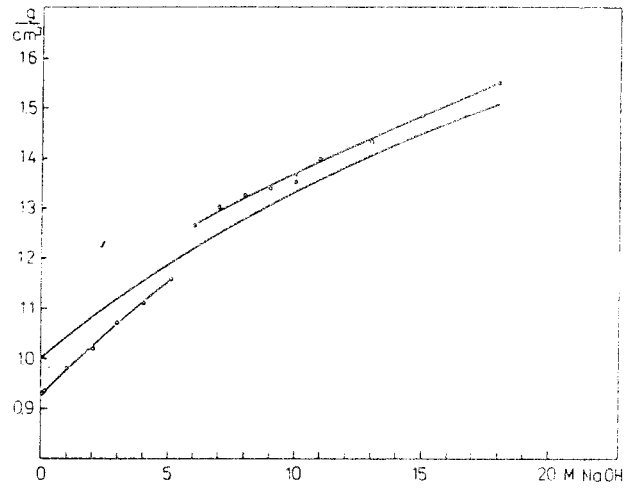


Fig. 2a Density of frozen NaOH solutions at 77 K vs the concentration (upper and lower curves). The continuous line without experimental points denotes the density of liquid solution at the room temperature (literature values).

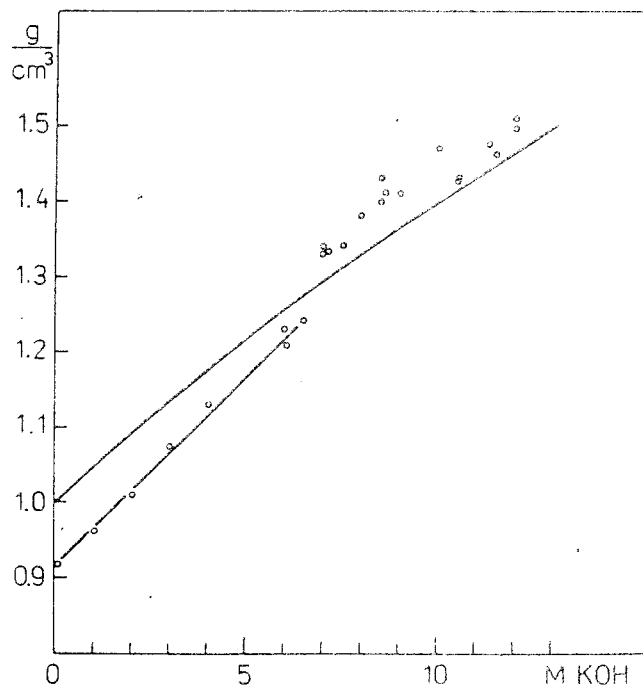


Fig. 2b Density of frozen KOH solutions vs the concentration. The continuous line without experimental points denotes the density of liquid solution at the room temperature.

Figure 3

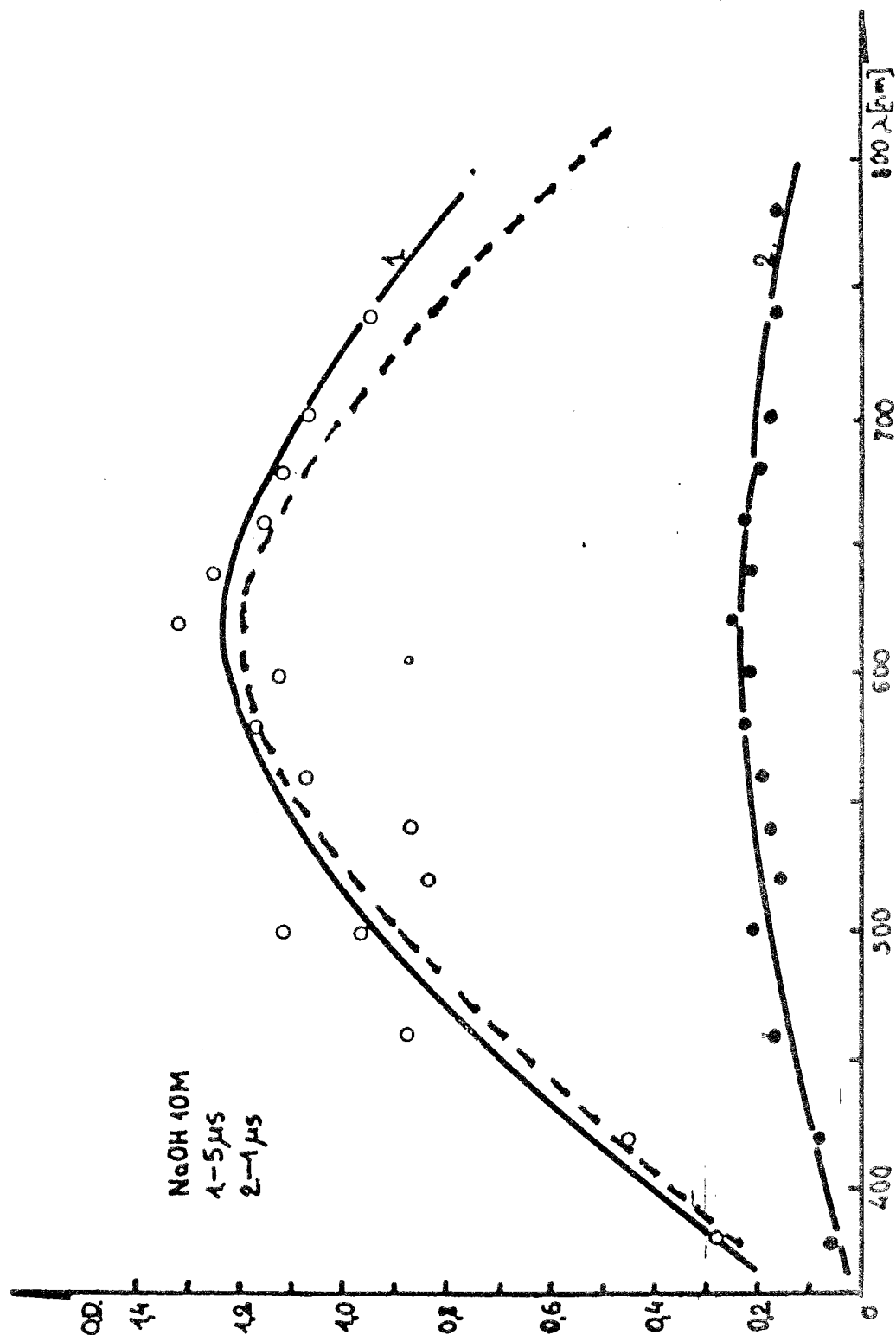


Figure 3. Comparison of  $e_t^-$  (glassy) spectra obtained by Cherenkov Method (continuous lines) and the conventional pulse radiolysis method (dotted line).

Figure 4

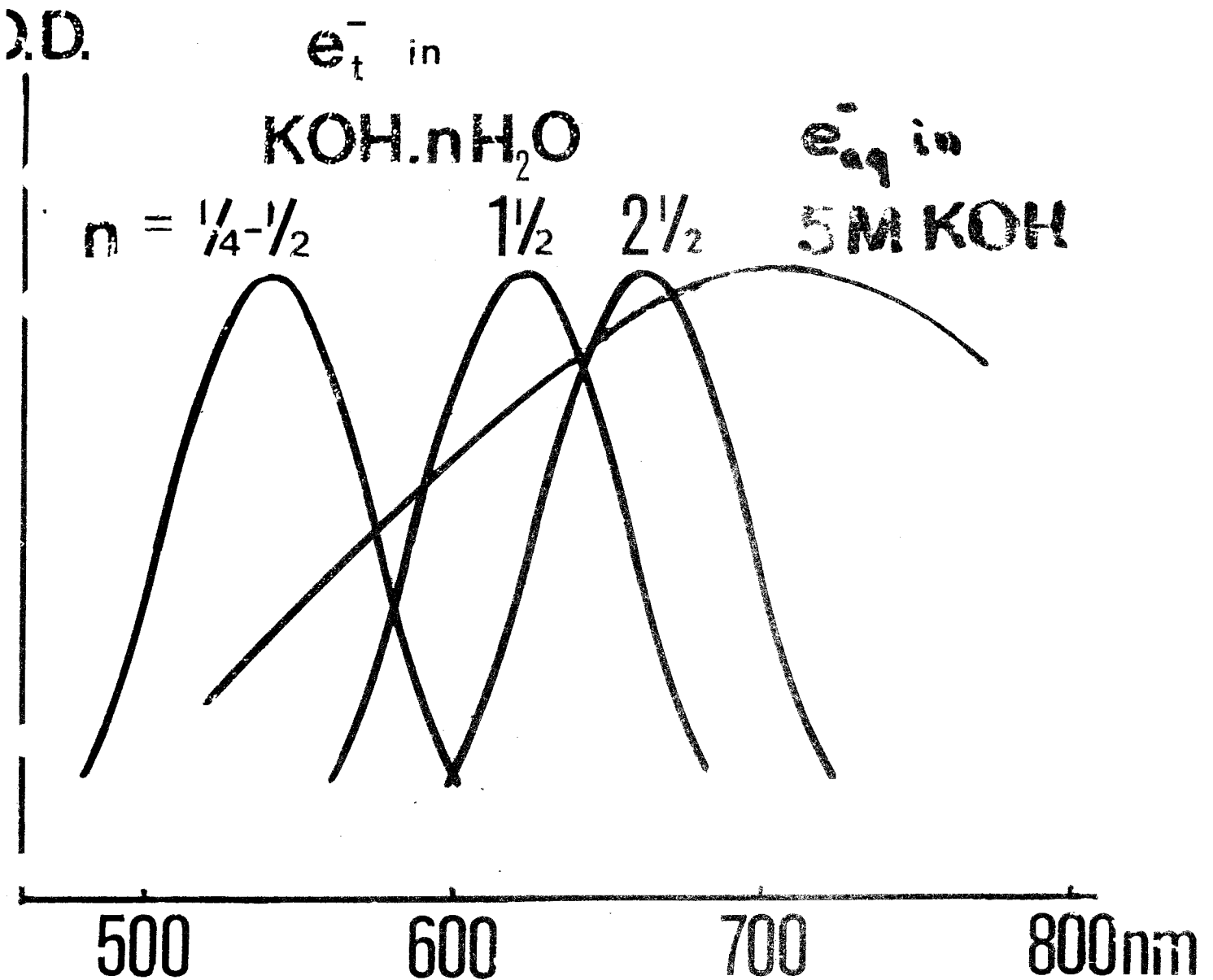


Figure 4. Comparison of normalized spectra of electron trapped in  $\text{KOH} \cdot n\text{H}_2\text{O}$  crystal hydrates with the spectrum of  $e_{aq}^-$  in  $5\text{M KOH}$  (liquid). All spectra at ambient temperature.

Figure 5

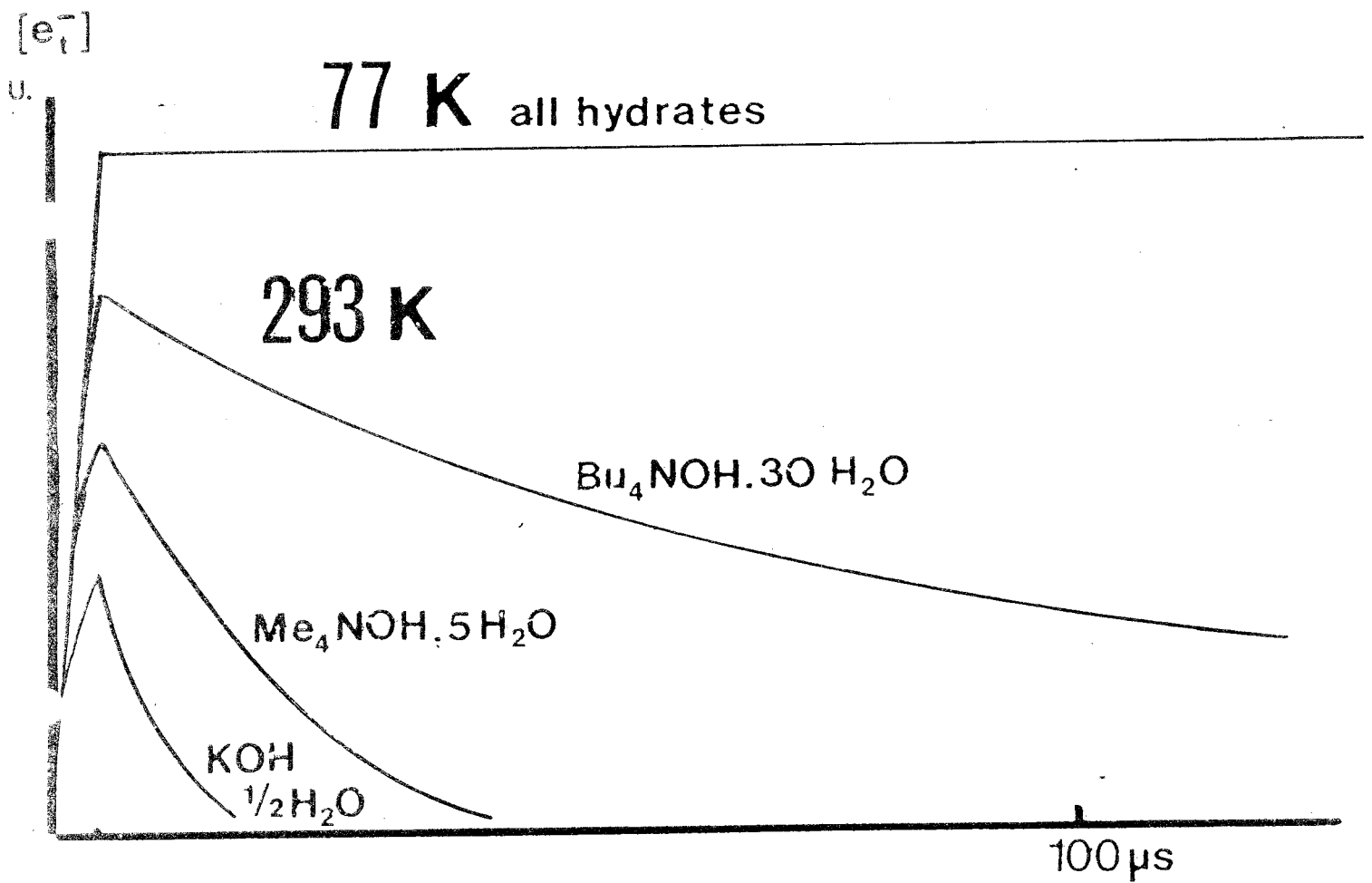


Figure 5. Rough estimate of  $e_t^-$  decay in different matrices.

Figure 6

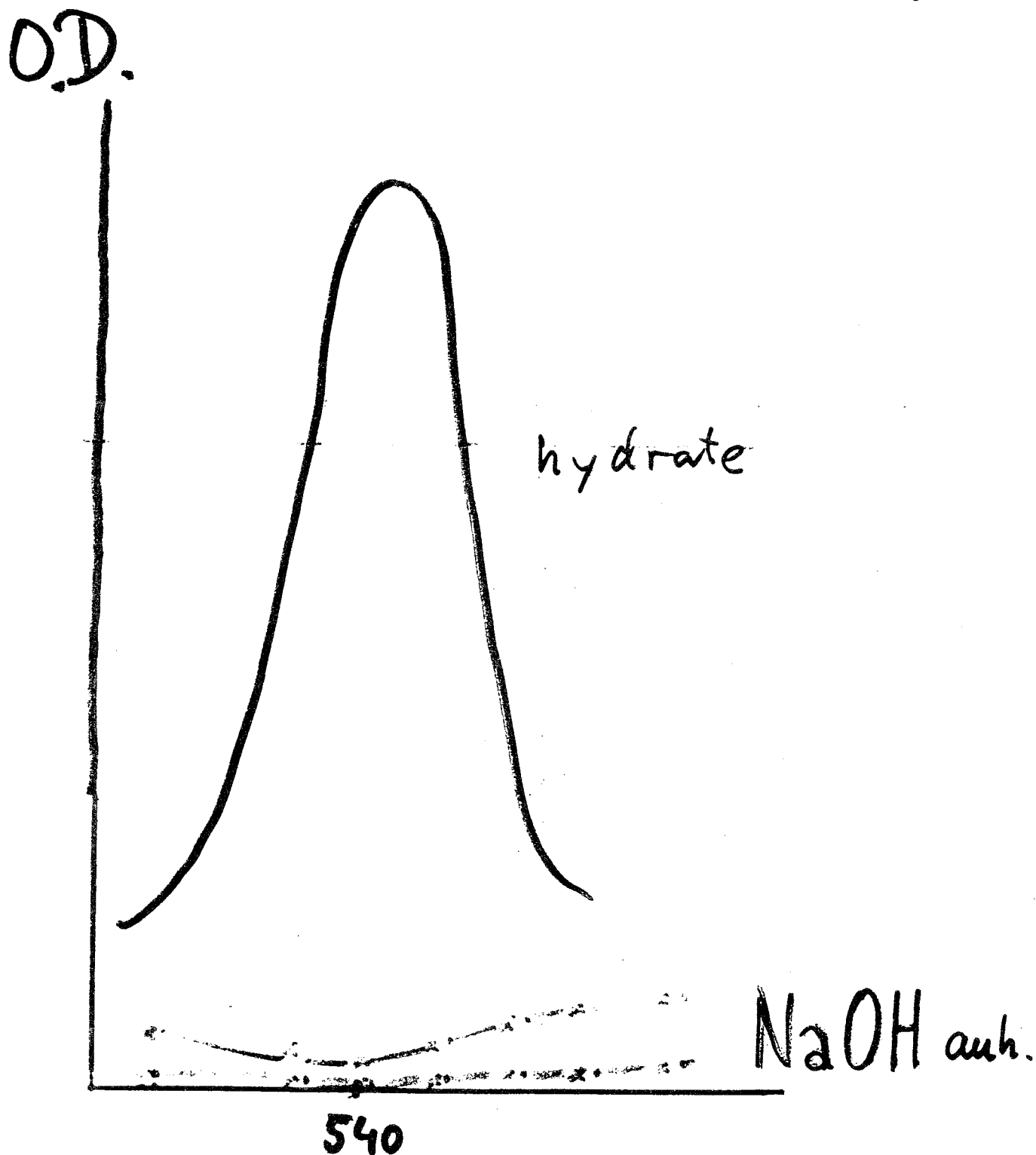
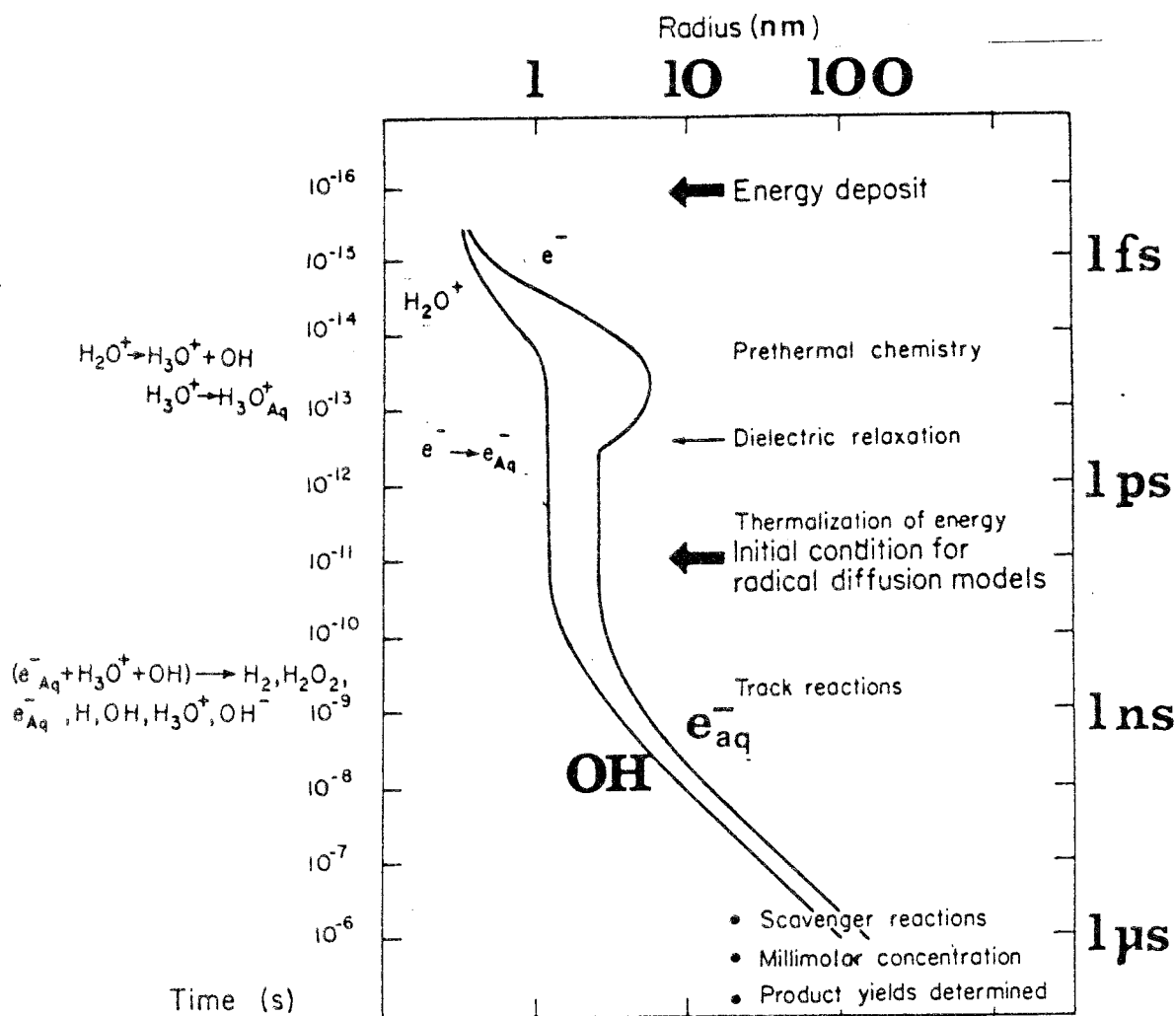


Figure 6. Spectrum of  $e_t^-$  in  $\text{NaOH}\cdot\text{H}_2\text{O}$  (decaying fast) and of  $e_t^-$  as F-center (permanent) in anhydrous  $\text{NaOH}^t$  (lower dotted curves). Ambient temperatures.



Figure 7



Space-time development of small isolated energy deposit (spur) in a dilute aqueous system

Figure 7. Space time development of small isolated energy deposit (spur) in a dilute aqueous system.

Figure 8

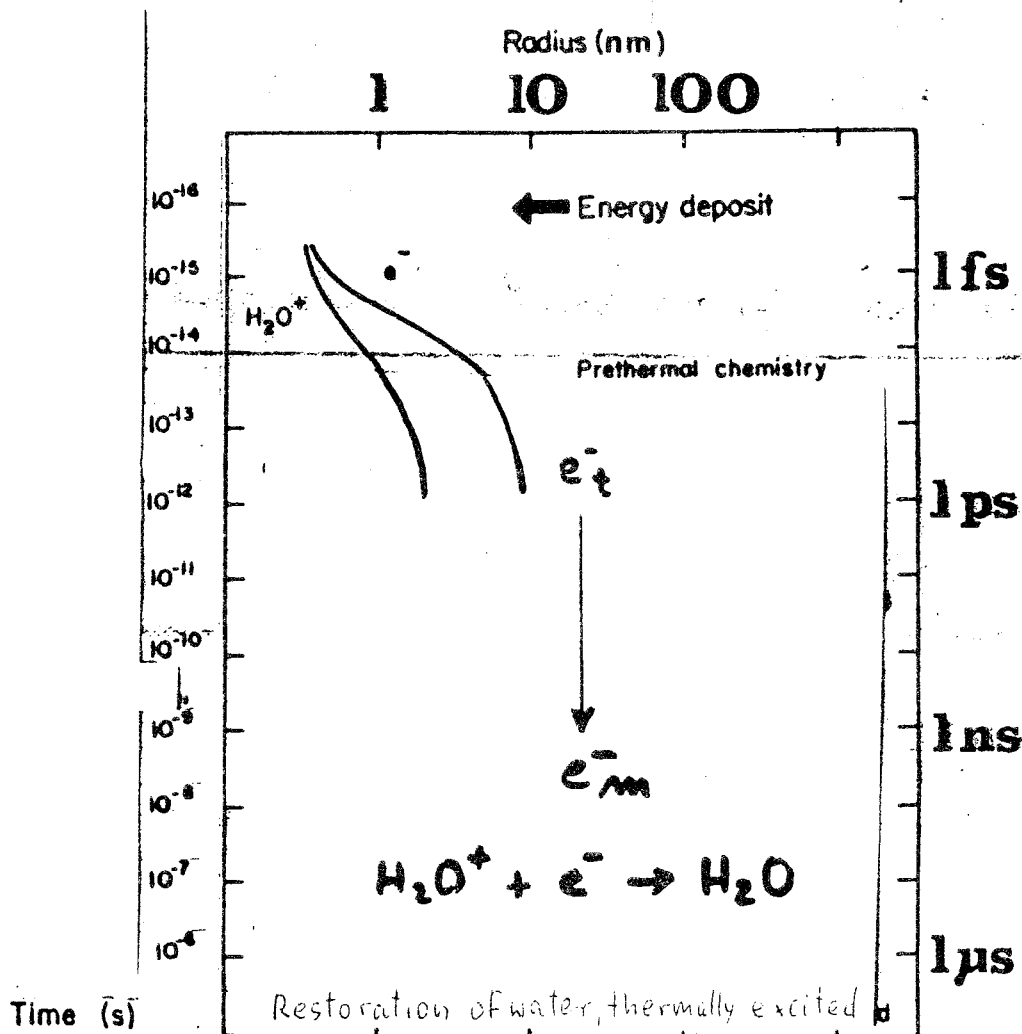


Figure 8. Proposed restoration of water at an early stage in solid crystalline phase.

## *List of KBS's Technical Reports*

1977-78

TR 121

**KBS Technical Reports 1 – 120.**

Summaries. Stockholm, May 1979.

1979

TR 79-28

**The KBS Annual Report 1979.**

KBS Technical Reports 79-01 – 79-27.

Summaries. Stockholm, March 1980.

1980

TR 80-26

**The KBS Annual Report 1980.**

KBS Technical Reports 80-01 – 80-25.

Summaries. Stockholm, March 1981.

1981

TR 81-17

**The KBS Annual Report 1981.**

KBS Technical Reports 81-01 – 81-16.

Summaries. Stockholm, April 1982.

1982

TR 82-28

**The KBS Annual Report 1982.**

KBS Technical Reports 82-01 – 82-27.

1983

TR 83-77

**The KBS Annual Report 1983.**

**KBS Technical Reports 83-01-83-76**

**Summaries. Stockholm, June 1984.**

1984

TR 84-01

**Radionuclide transport in a single fissure**

**A laboratory study of Am, Np and Tc**

Trygve E Eriksen

Royal Institute of Technology

Stockholm, Sweden 1984-01-20

TR 84-02

**Radiolysis of concrete**

Hilbert Christensen

Studsvik Energiteknik AB,

Nyköping, Sweden

Erling Bjergbakke

Risø National Laboratory,

Roskilde, Denmark 1984-03-16